LINE-A

GEOLOGY

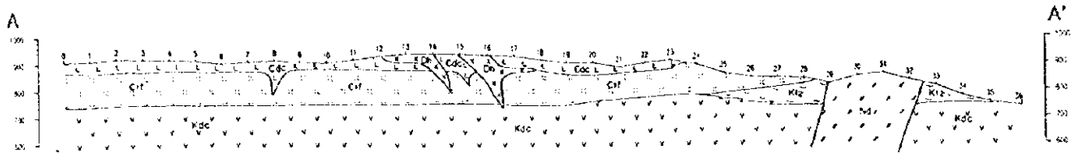

CHARGEABILITY

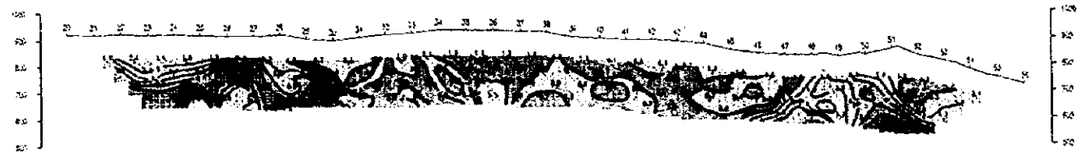

RESISTIVITY

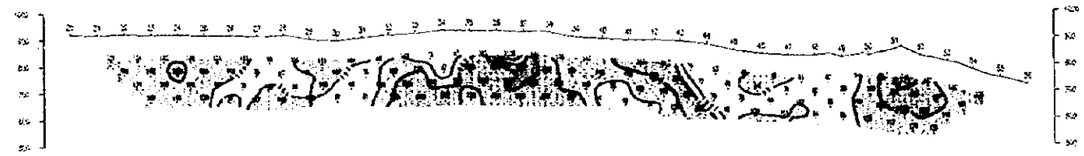

LINE-B

GEOLOGY

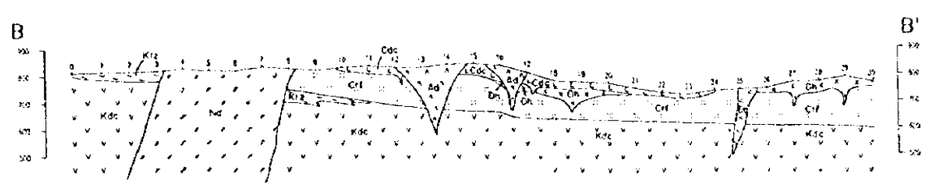

CHARGEABILITY

RESISTIVITY

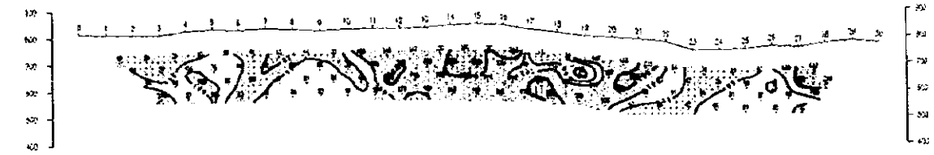

LINE-C

GEOLOGY

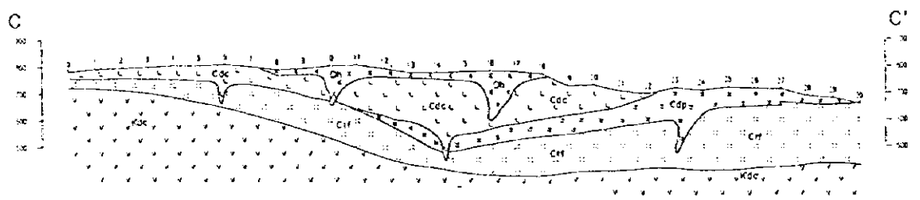

CHARGEABILITY

RESISTIVITY

LINE-E

GEOLOGY

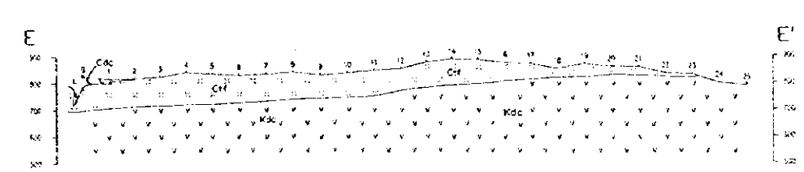

CHARGEABILITY

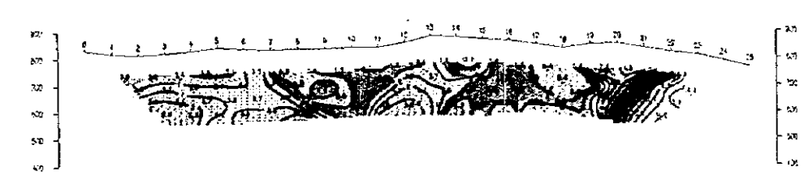

RESISTIVITY

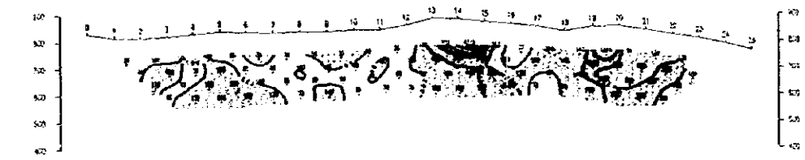

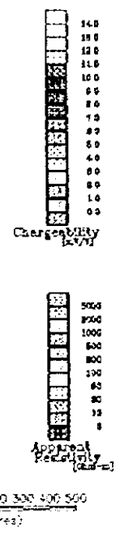

Fig.II-3-11 IP Sections of Apparent Resistivity and Chargeability (Line A,B,C,E of Phase I Survey)

LINE-D

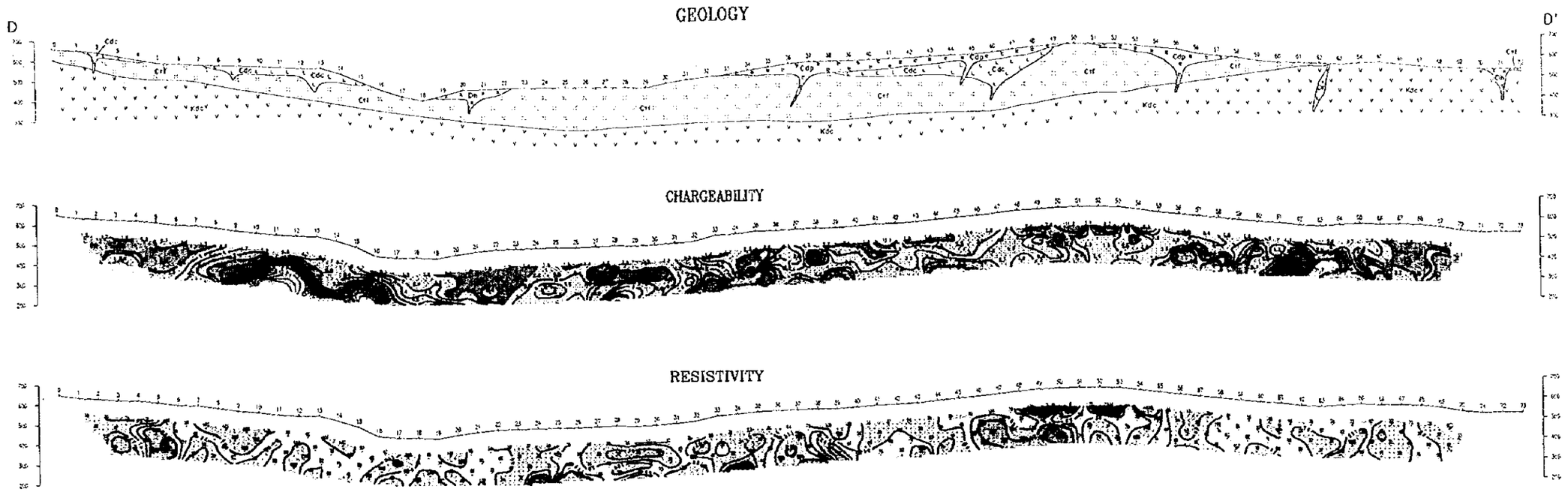

LINE-F

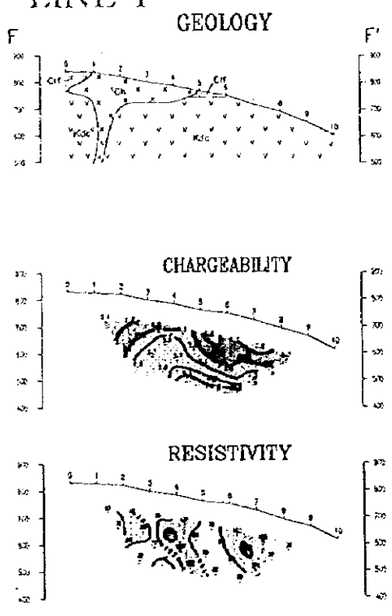

LINE-G

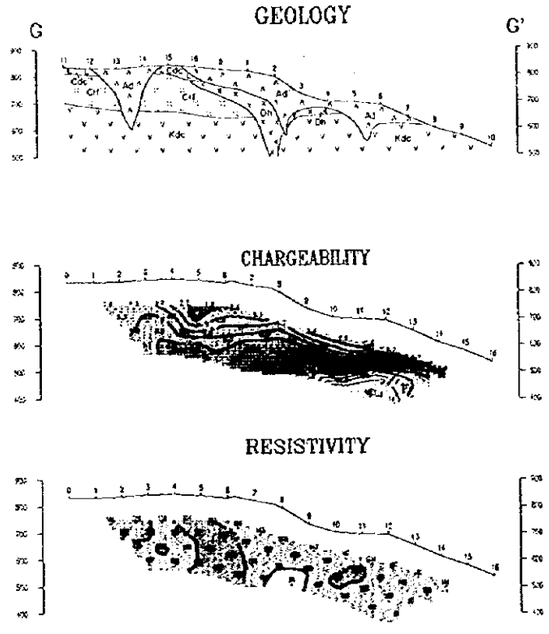

LINE-H

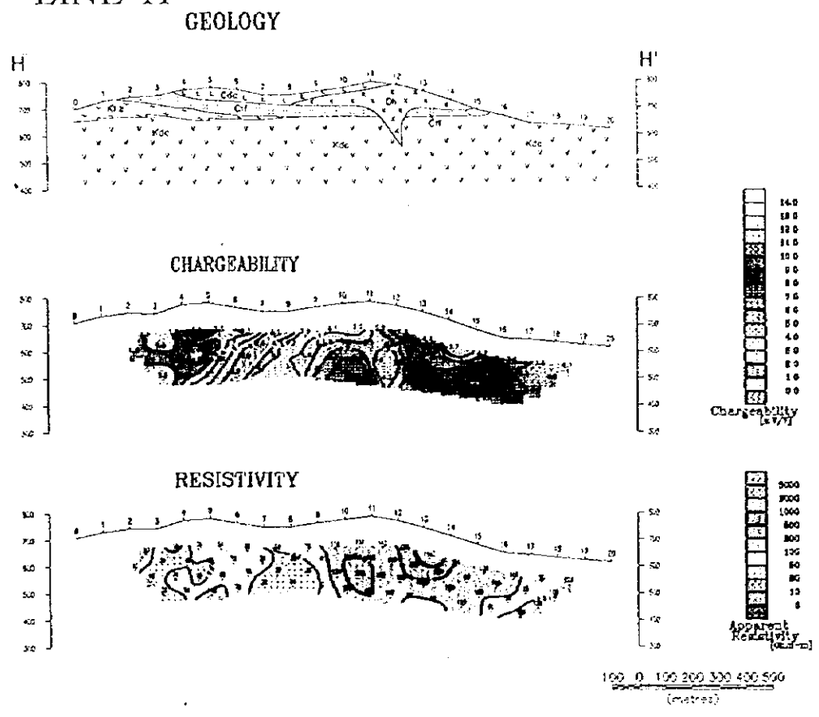

Fig.II-3-12 IP Sections of Apparent Resistivity and Chargeability (Line D,F,G,H of Phase I Survey)

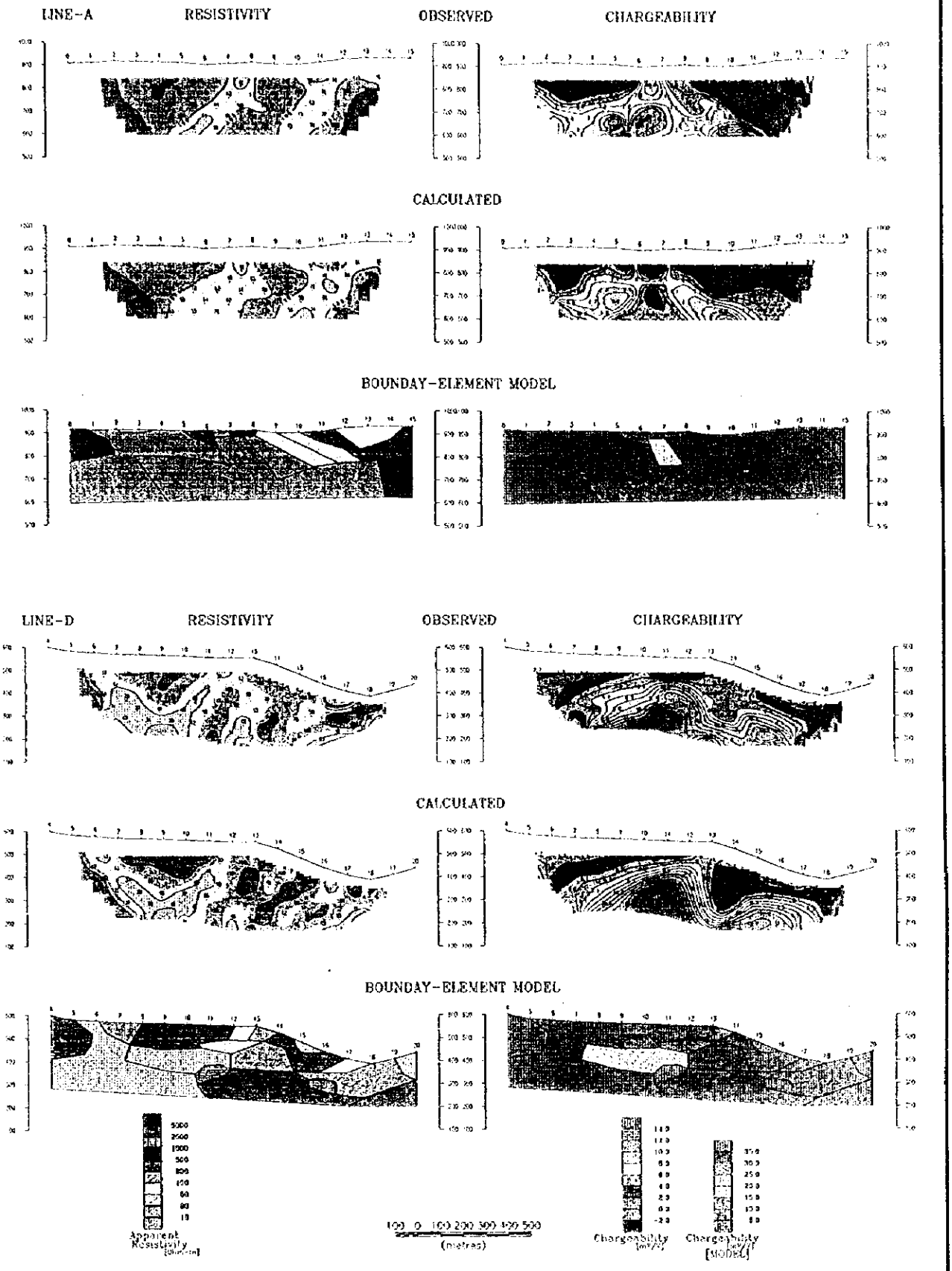

Fig.II-3-13 IP Sections of Simulated Result (Line A,D of Phase I Survey)

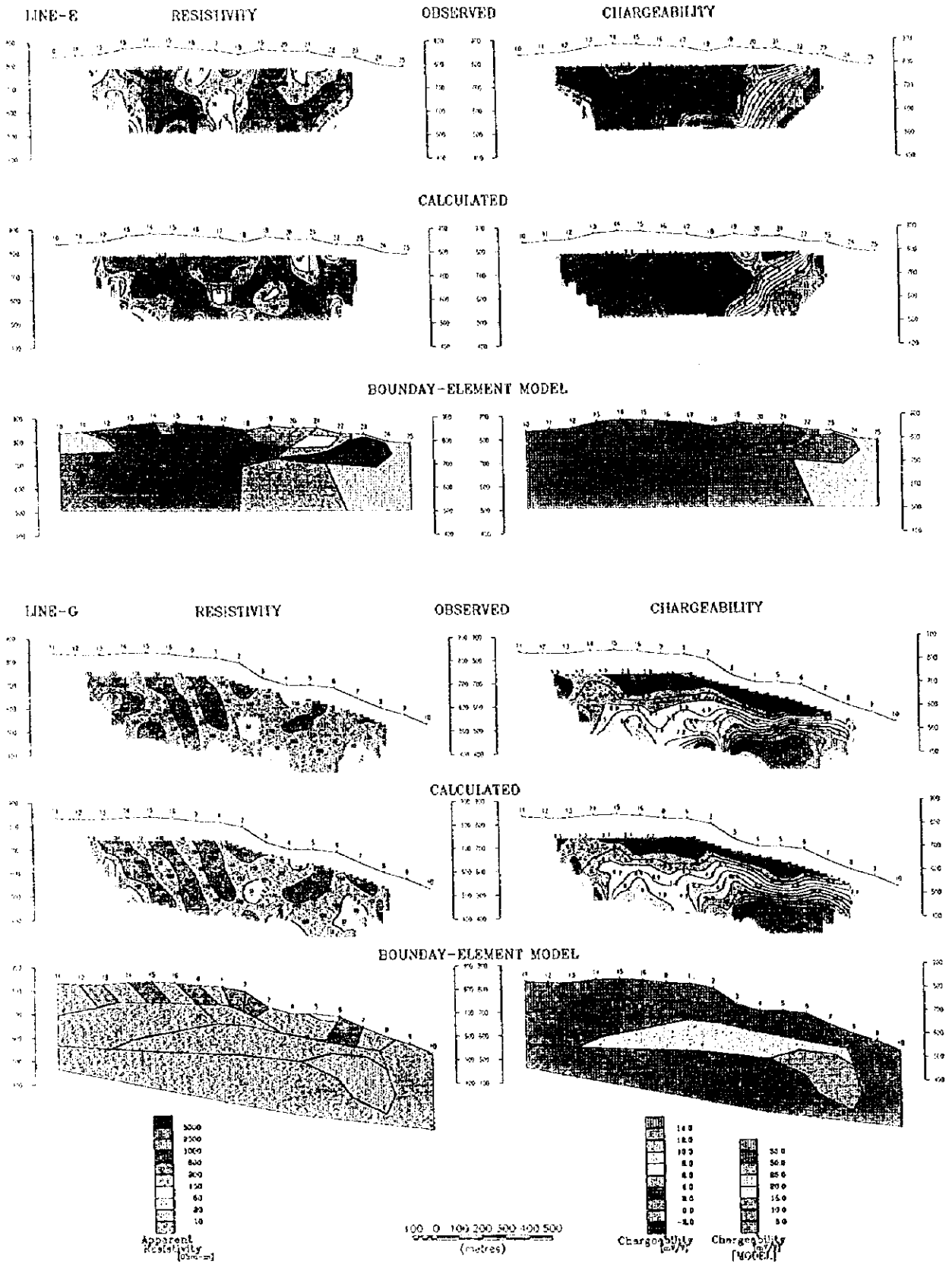

Fig.II-3-14 IP Sections of Simulated Result (Line E,G of Phase I Survey)

2) Phase II (1996)

(1) Results of the Survey

Survey line and locations are shown in Fig.II-3-22.

Results of the survey are summarized as shown in Fig.II-3-15~19 and Table II-3-7.

Table II-3-7 Results of IP Survey (Phase II)

Survey Line	Apparent Resistivity (Ω·m)	Chargeability (mV/V)	Characteristics of IP Distribution Pattern
A	14~729	-1.7~31.7	Around No.20~25 more than 10mV/V. Clear IP anomaly like pantaloon shape.
B	25~970	-4.4~30.4	Around No.20~30 more than 10mV/V. Clear IP anomaly.
C	24~704	-0.9~26.0	Around No.4 more than 10mV/V IP anomaly like pantaloon shape. Around Nos.24~30 more than 10mV/V Clear IP anomaly.
D	79~992	-1.7~12.8	Around Nos.0~1 and 10 Weak IP anomaly.
E	135~1,419	-0.4~11.0	Around Nos.0~1 Weak IP anomaly At depth of Nos.4~8 Weak IP anomaly
F	24~289	1.0~19.9	Around Nos.5~12 more than 10mV/V Clear IP anomaly.
G	19~338	0.3~16.9	Around Nos.11~13 more than 10mV/V Clear IP anomaly.
H	18~288	0.4~16.1	At depth of No.10 more than 10mV/V Clear IP anomaly.
I	12~927	-1.0~18.1	At depth of Nos.12,15 more than 10mV/V Clear IP anomaly.
J	3~497	0.8~4.6	No anomaly.
K	9~993	0.8~5.0	No anomaly.
L	12~353	0.3~7.4	No anomaly.
M	9~543	0.8~6.6	No anomaly.
N	12~351	0.7~10.4	Around Nos.5~6 extremely weak IP anomaly like pantaloon shape.

(2) Results of analysis

Results of analysis are summarized as shown in Fig.II-3-20~22 and Table II-3-8.

Table II-3-8 Summary of IP Survey (Phase II)

Survey Line	Estimated Resistivity & Chargeability of Origin of IP Anomaly	Estimated Distribution Pattern of Origin of IP anomaly
A Killik area	150~750 Ω·m & 40mV/V 100 Ω·m & 100mV/V 300 Ω·m & 90mV/V	·It developes at deeper part than 100m. Distribute widely. Extremely weak mineralization was assumed. ·At deeper place than 100m of No.25 siliceous ore was assumed.
D Kepçelik area		It developes at deeper part than 150m. Extremely weak mineralization was assumed. The state of distribution was not clear.
F Taflancık area	40 Ω·m & 40mV/V	It developes at deeper part than 100m. Siliceous ore was assumed.
H Taflancık area	60 Ω·m & 50mV/V	It developes at deeper part than 150m. Extremely weak mineralization was assumed. Widely distribute flatly.
I Taflancık area	3 Ω·m & 40mV/V	It developes at deeper part than 150m. Mineralization was assumed relatively in a good state.

(3) Consideration

The present survey clarified a distribution of the IP anomaly zone in Taflancık area extracted in the previous year. Also, a new IP anomaly zone was observed in Killik area.

The results were obtained that a high resistivity zone of 300 Ω·m or more among resistivity of n = 1 representing nearby surface obtained from the survey results corresponds well to intrusive rocks. However, the resistivity, on the whole, changes according to a degree of mineralization and argillization in a resistivity zone of approx. 200 Ω·m or less due to intrusive rocks, a difference in lithology of the Kızılkaya and Çağlayan Formation. A low resistivity zone of approx. 40 Ω·m or less corresponds well to argillic alteration on surface.

· Killik Area

A clear chargeability anomaly distributed in a wide area which was the greatest around No. 25 on

each survey line was observed in Killik area.

The anomalous chargeability maximum 30mV/V was in a distribution area of dacite lava in the Kızılkaya Formation.

According to the simulation analysis, the strongest anomaly source is considered to be a siliceous ore with a resistivity of 100 Ω·m and a chargeability of 100mV/V at a depth of 100m or more at No. 25. It is thought that a weak mineralized area is widely distributed on its periphery.

Considering this IP anomaly distribution and the IP effect affected by a steep landform, it is thought that a strong IP anomaly source has not been grasped yet in the present survey.

· Kepçelik Area

A similar weak anomaly was observed on the end of each survey line in Kepçelik area.

According to the simulation analysis results, it is presumed that a resistivity is 300 Ω·m and a chargeability is 90mV/V at a depth of about 100m or more at No.3 as an anomaly source. Since this is an anomaly source calculated from an IP anomaly value at the end of the survey line, the distribution condition and other data are not clear. It is possible that this reflects a very weak mineralization.

· Taflancık Area

An IP anomaly was observed on each survey line in Taflancık area. Farther we go north, stronger the tendency is that the IP anomaly distribution extends in the NNE-SSW direction in the depth.

According to the simulation analysis, it is presumed that there are anomaly sources with a resistivity of 40 Ω·m and a chargeability of 40mV/V at a depth of about 100m or more of Nos. 8 to 14 on survey line F, with a resistivity of 60 Ω·m and a chargeability of 50mV/V at a depth of 150m or more of Nos. 4 to 11 on survey line H, and with a resistivity of 3 Ω·m and a chargeability of 40mV/V at a depth of 150m or more of Nos.10 to 14 on survey line I, respectively.

The weak mineralization was expected on all the survey lines and it is considered to be relatively favorable on the survey line I.

· Çalkaya area

An anomaly in chargeability peculiar to each lines was not observed in Çalkaya area.

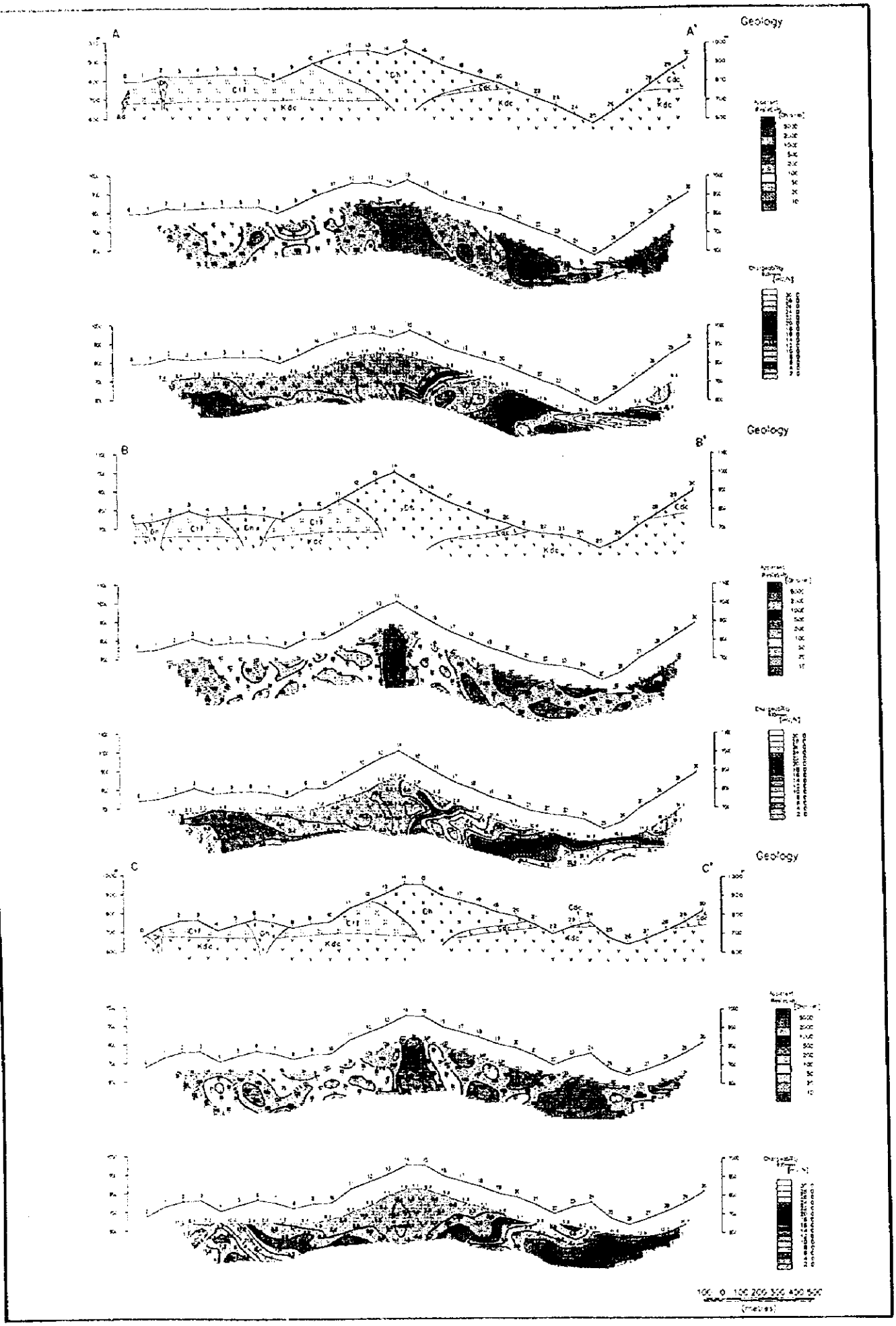

Fig.II-3-15 IP Sections of Apparent Resistivity and Chargeability Killik Area (Line A,B,C)

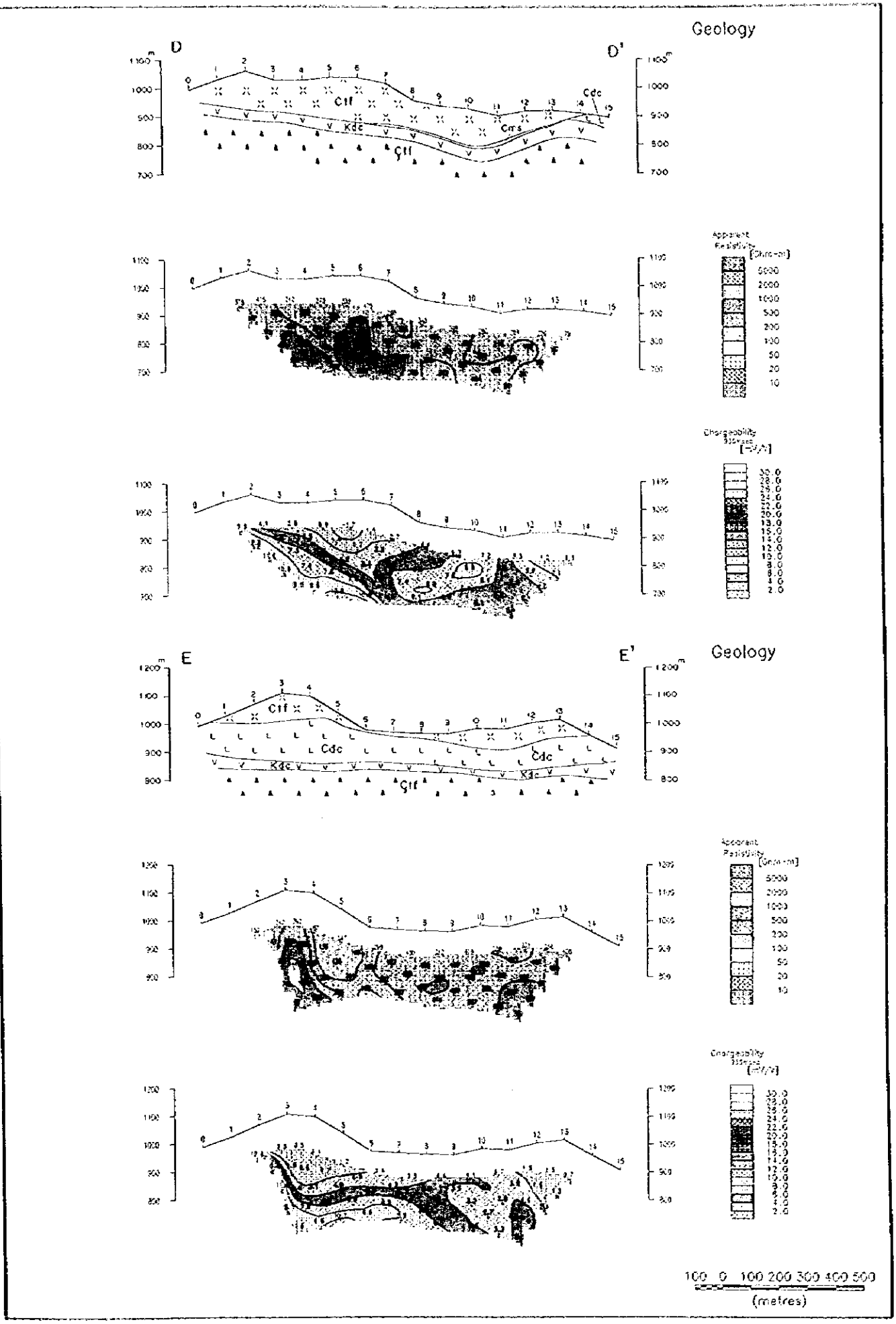

Fig.II-3-16 IP Sections of Apparent Resistivity and Chargeability Kepçelik Area (Line D,E)

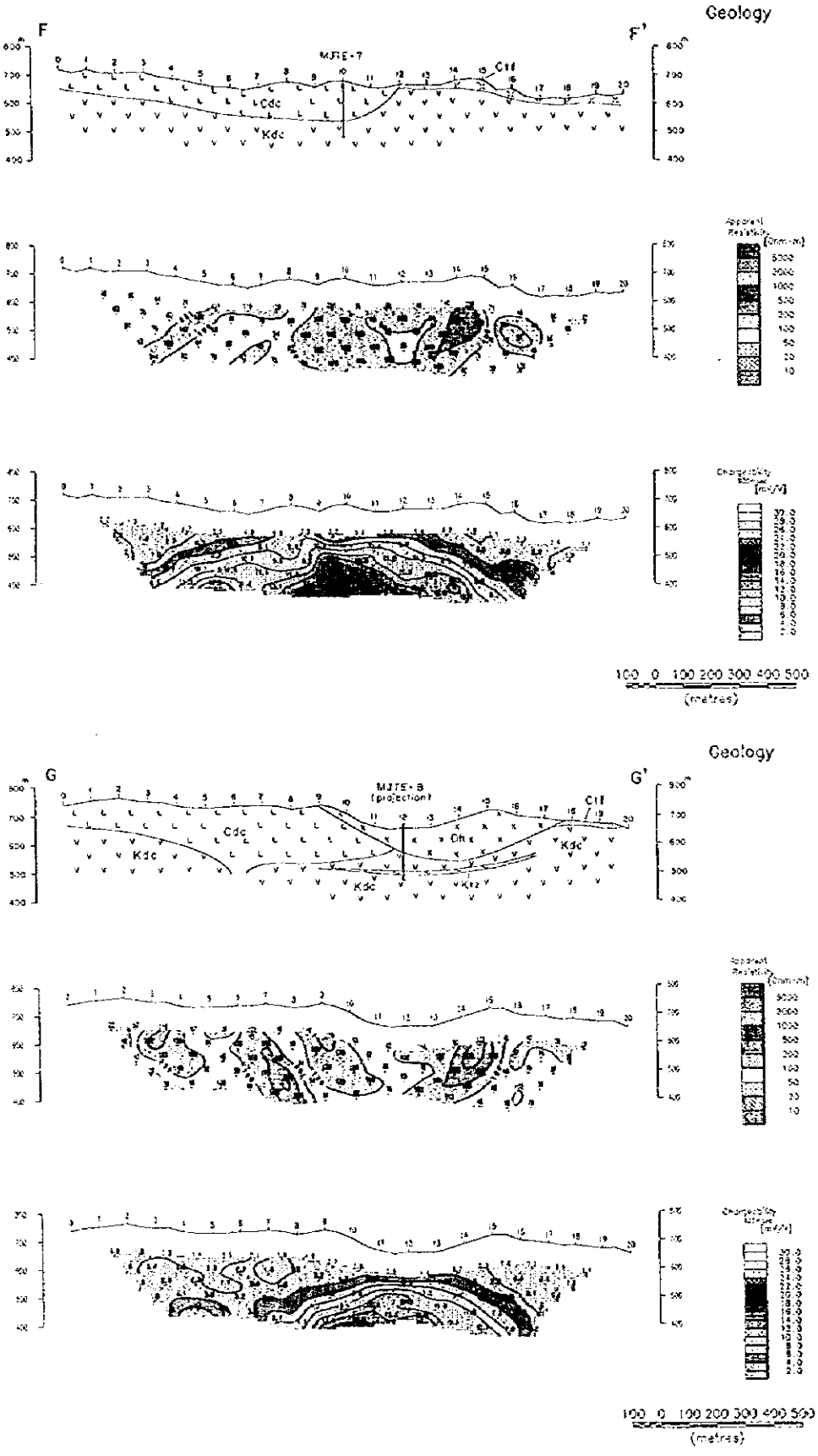

Fig.II-3-17 IP Sections of Apparent Resistivity and Chargeability Taflancık Area (Line F,G)

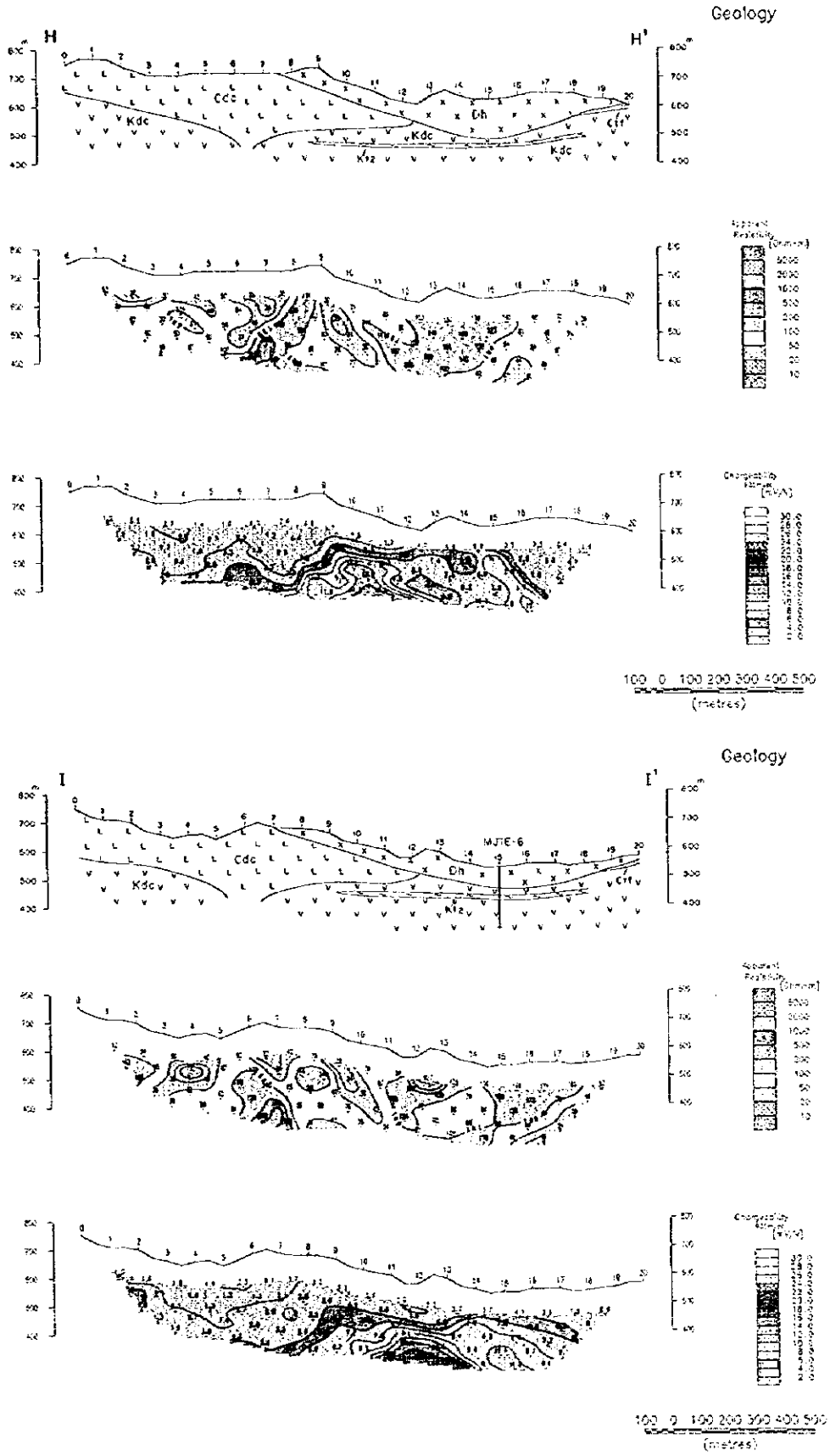

Fig.II-3-18 IP Sections of Apparent Resistivity and Chargeability Taflancık Area (Line H,I)

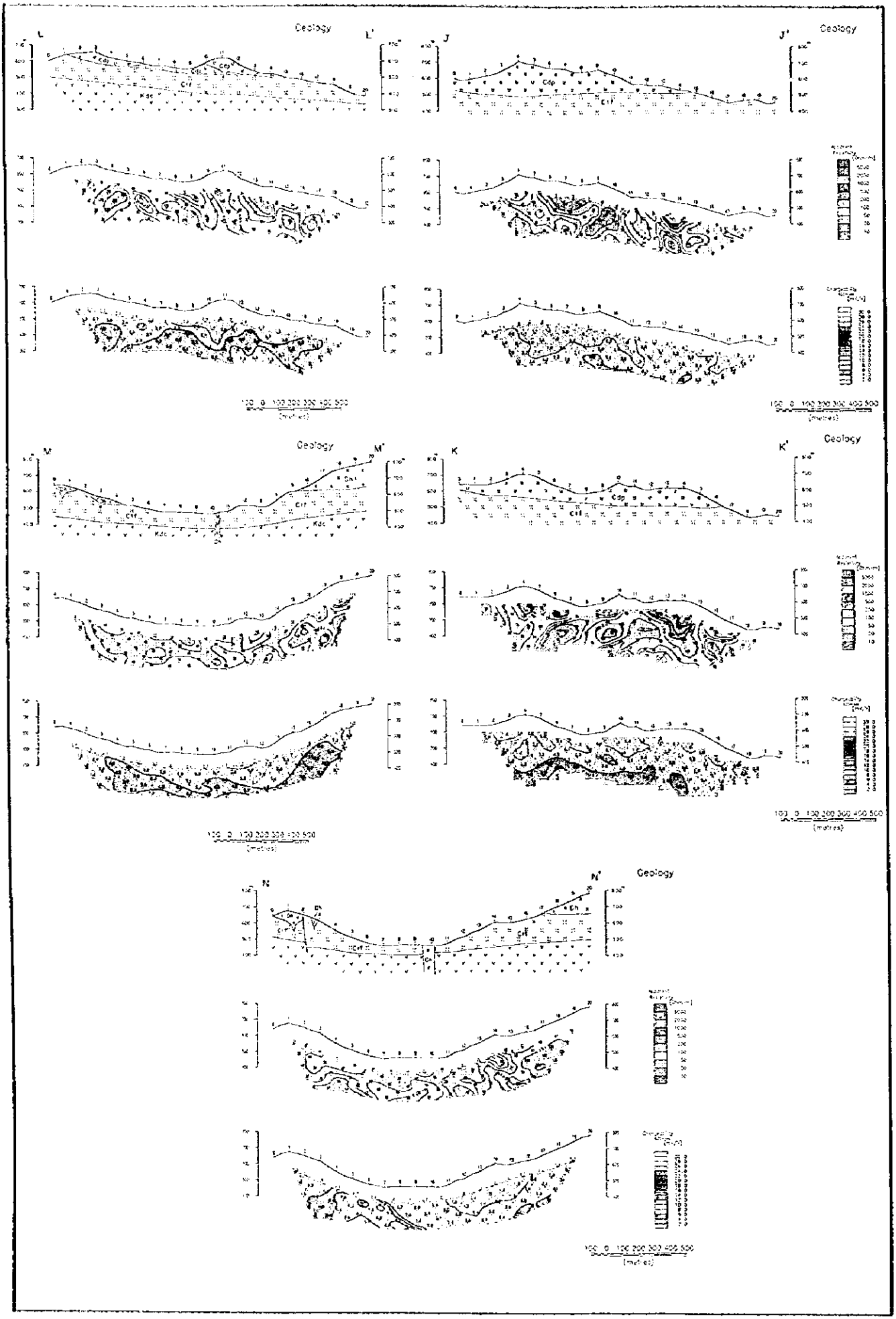

Fig.II-3-19 IP Sections of Apparent Resistivity and Chargeability Çalkaya Area (Line J,K,L,M,N)

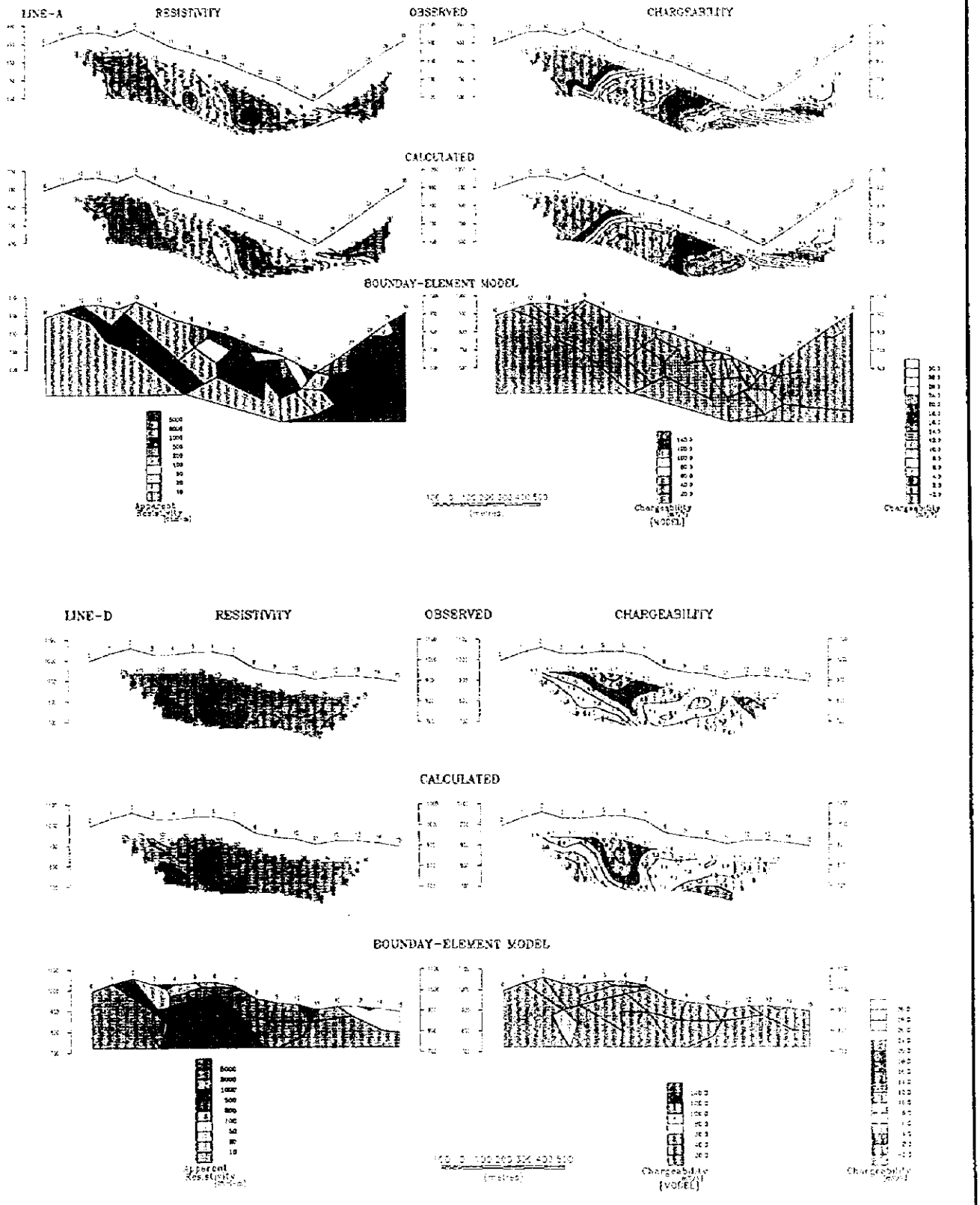

Fig.II-3-20 IP Sections of Simulated Result (Line A,D of Phase II Survey)

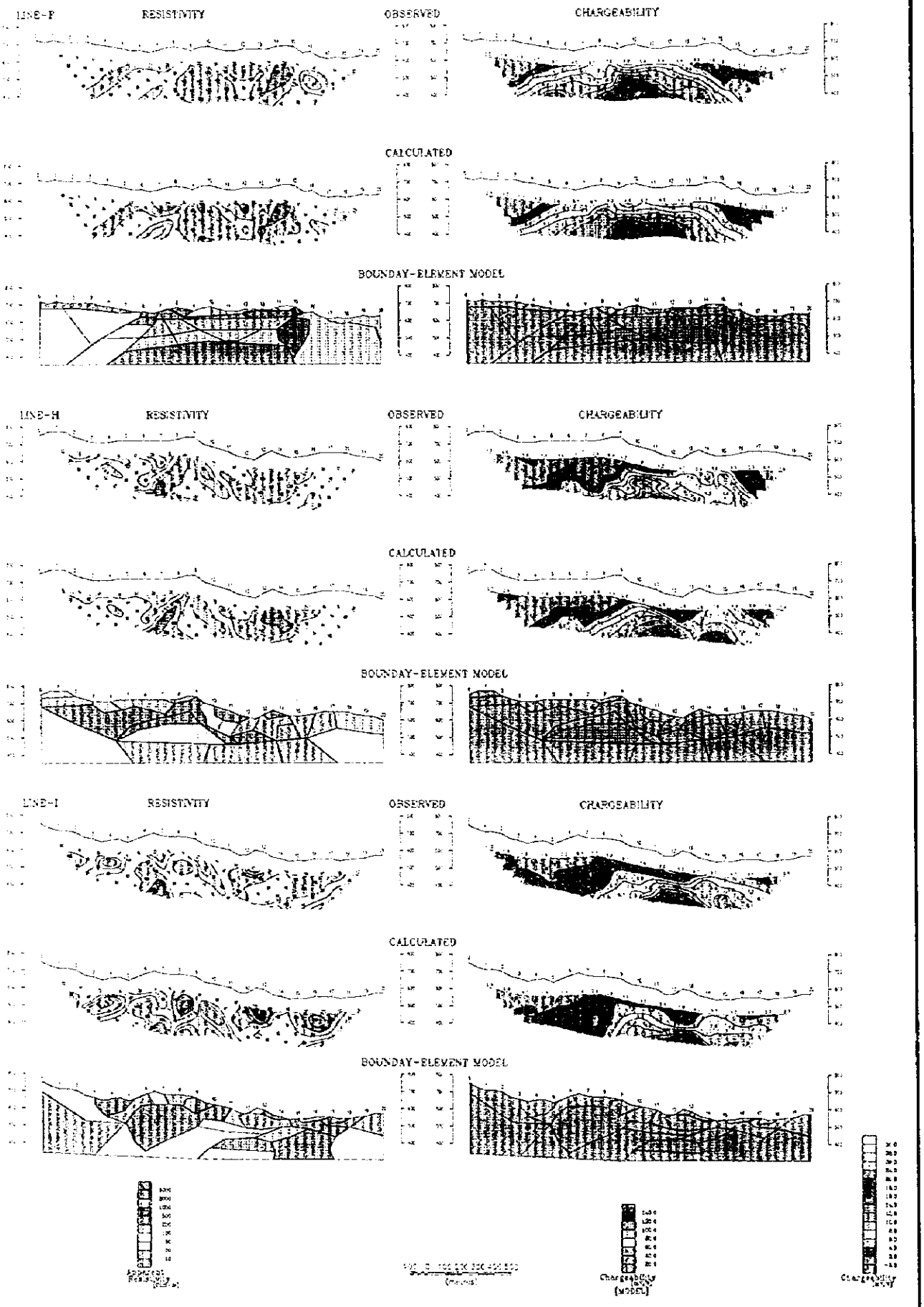

Fig.II-3-21 IP Sections of Simulated Result (Line F,H,I of Phase II Survey)

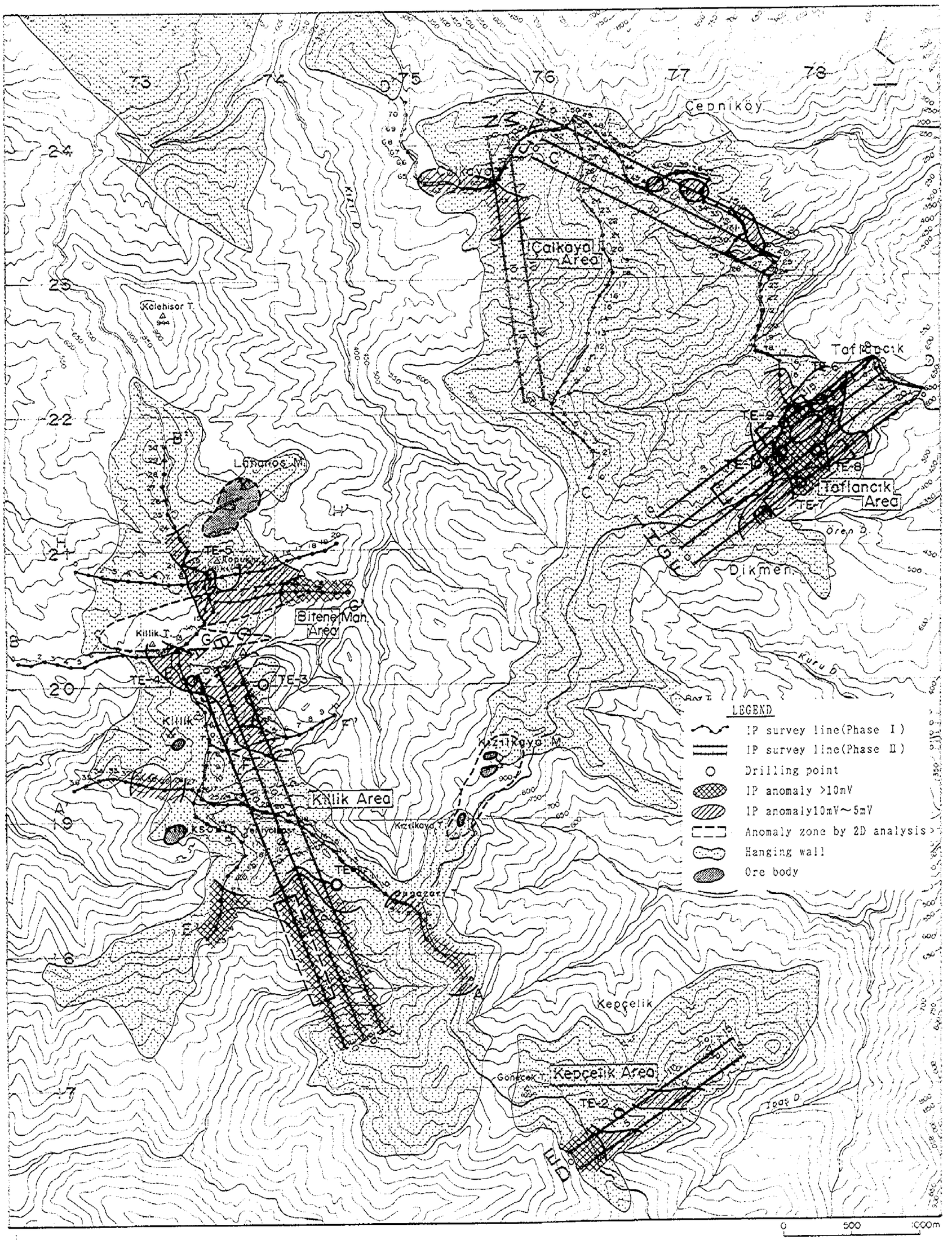

Fig.II-3-22 Summarized Map of IP Survey in Lahanos-Taflancık Area

3) Phase III (1997)

(1) Results of the survey

The results of the survey are shown in Fig.II-3-23~24 and Table II-3-9

Table II-3-9 Results of IP Survey (Phase III)

Survey Line	Apparent Resistivity (Ω·m)	Chargeability (mV/V)	Characteristics of IP Distribution Pattern
A	4 ~ 405	0.6 ~ 7.6	A tendency of high chargeability in high resistivity part. No anomaly.
B	10 ~ 440	-0.8 ~ 4.9	A tendency of high chargeability in high resistivity part. No anomaly.
C	9 ~ 181	1.1 ~ 4.3	Tendency of resistivity distribution is almost similar to line B. No anomaly.
D	5 ~ 608	-2.9 ~ 9.8	In site Nos.20-22, definite but weak chargeability anomaly.
E	15 ~ 207	-0.1 ~ 7.5	Weak but clear anomaly in site Nos.6-8 near Karaerik and Krılar.
F	6 ~ 352	0.5 ~ 8.9	A tendency of high chargeability in high resistivity part. No anomaly.
G	14 ~ 213	0.8 ~ 7.8	A tendency of high chargeability corresponding to high resistivity No anomaly.

(2) Results of Physical Property Test

The relationship between the apparent resistivity and chargeability for each of all the samples (1st year through 3rd year) and the relationship between each sample and MF are shown in Fig. II-3-25 and Fig.II-3-26 respectively.

Of all the samples, with respect to the rocks other than the ores, the dissemination sample of pyrite in dacite lava (Kızılkaya Formation) showed chargeability of more than 20mV/V. The samples high resistivity tend to exhibit high chargeability.

On the basis of MF, the rocks and ores are definitely separated by about 100, but those ranging from 100~1,000, belong to the category of weak siliceous ore to low grade black ore.

(3) Results of analysis

Results of analysis are summarized as shown in Fig.II-3-27~30 and Table II-3-10.

Table II-3-10 Summary of IP Survey (Phase III)

Measuring Line	Site No.	Result of Analysis
A	Nos. 8~16 Nos. 2~8, 14	No anomaly reflecting no mineralization. Shallow level: Mainly hard and massive hematite dacite. Shallow to deep level: Clay rich tuff. MF40at a maximum.
B	Nos. 18~24	No anomaly reflecting no mineralization. Hematite dacite continues to deep level. MF: 40 at a maximum.
C		No anomaly reflecting no mineralization. Mostly low less than 30 Ω·m. MF: 40 at a maximum.
D	Nos. 8~12 Nos. 20~24 Nos. 6~8,19	In general, resistivity varies in a short interval Deep level: High resistivity and high chargeability. Shallow level: High resistivity and high chargeability (hematite dacite). Vicinities of Karaelik and Karılar ore deposits: Weak anomaly of chargeability. MF: 65 at near depth of 150m in site No.8; 90 at a maximum at depth of 50m or more in site No. 20.
E	Nos. 4~6 No. 19	Low resistivity and high chargeability near Karaelik deposit. Hight resistivity and weak anomaly of chargeability in the eastward extension of Karılar deposit. MF: 100 at a maximum at depth of about 50m near Karaelik ore deposit.
F	Nos. 8~18 Nos. 22~24 No. 27	In general, high chargeability/high resistivity. There is the possibility that the high resistivity region of 100 Ω·m or more ranging from shallow level to deep level is a hematitic dacite integrally formed with those within measuring lines E and G? Lithofacies of high resistivity of 1,000 Ω·m or more at deep level is not determined. MF: 200 up to depth of 100 m. Weak mineralization of the Kızılkaya Formation.
G		No anomaly reflecting no mineralization. In general, high resistivity / high chargeability. MF: 40 at a maximum.

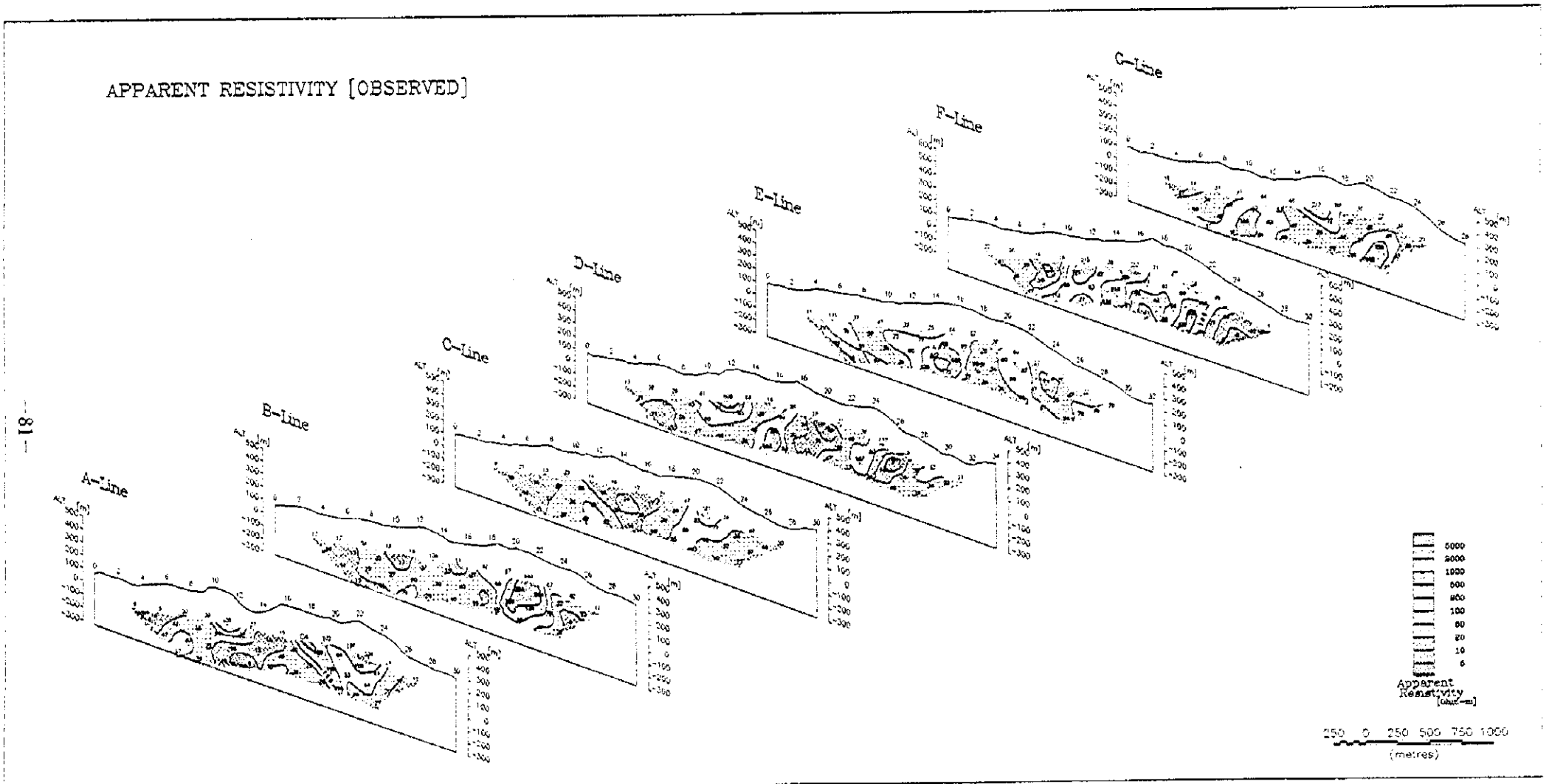

Fig.II-3-23 IP Sections of Apparent Resistivity (Karılar Area)

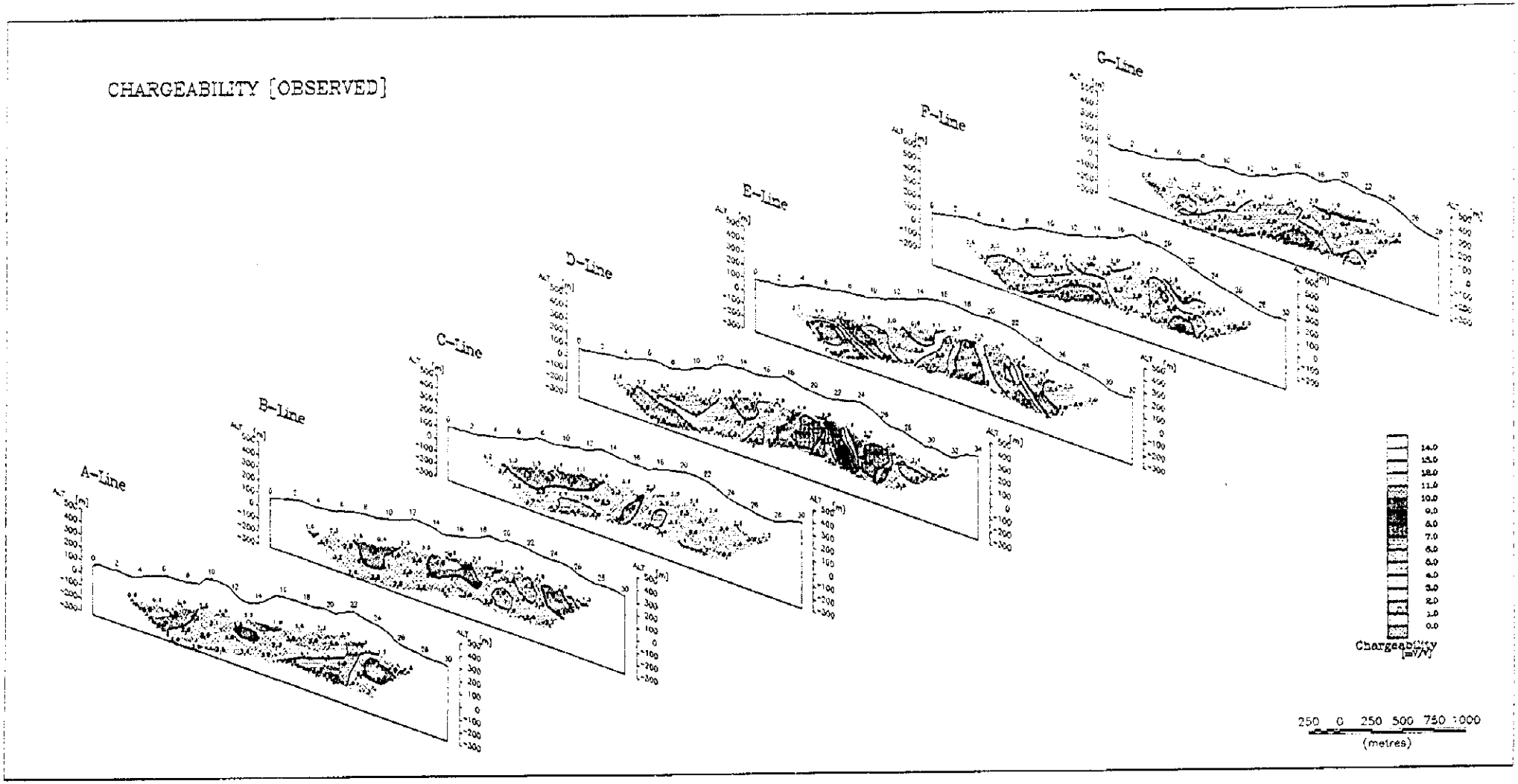

Fig.II-3-24 IP Sections of Apparent Chargeability (Karılar Area)

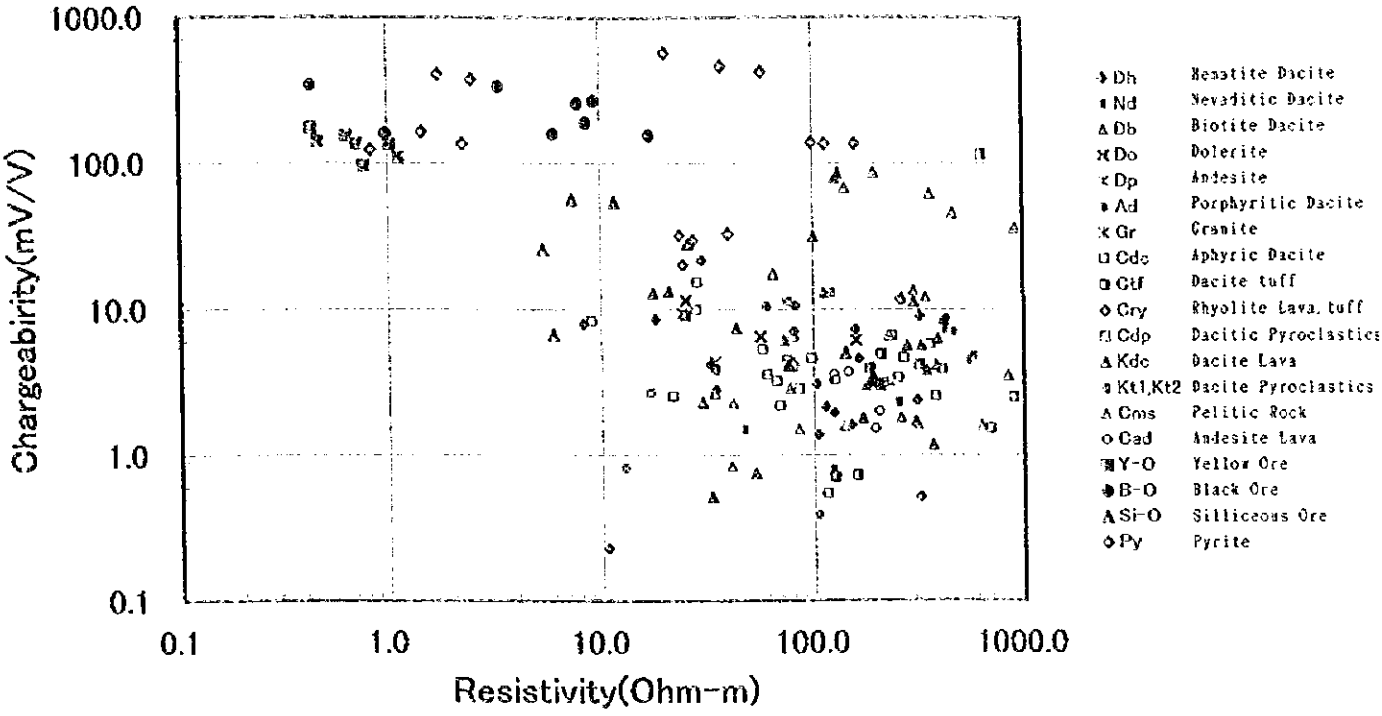

Fig.II-3-25 Relation between Apparent Resistivity and Chargeability of Rock and Ore Samples

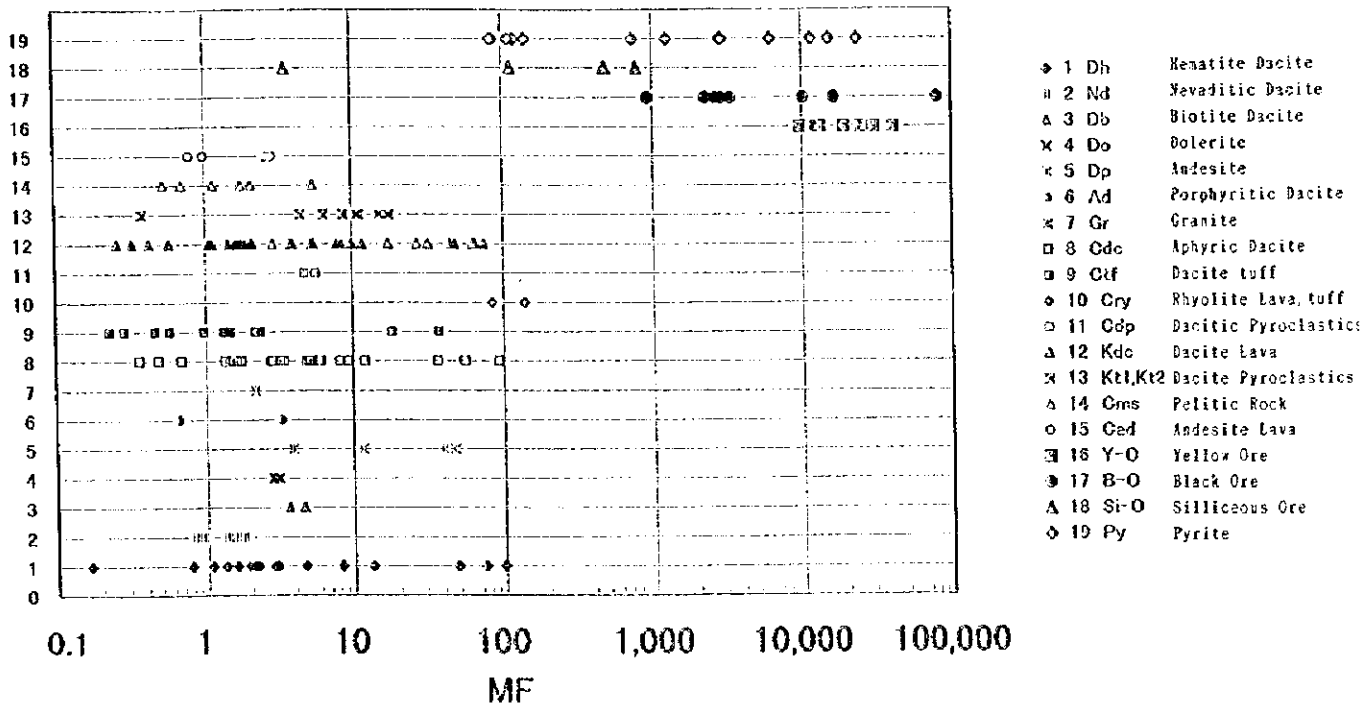

Fig.II-3-26 MF Property of Rock and Ore Samples

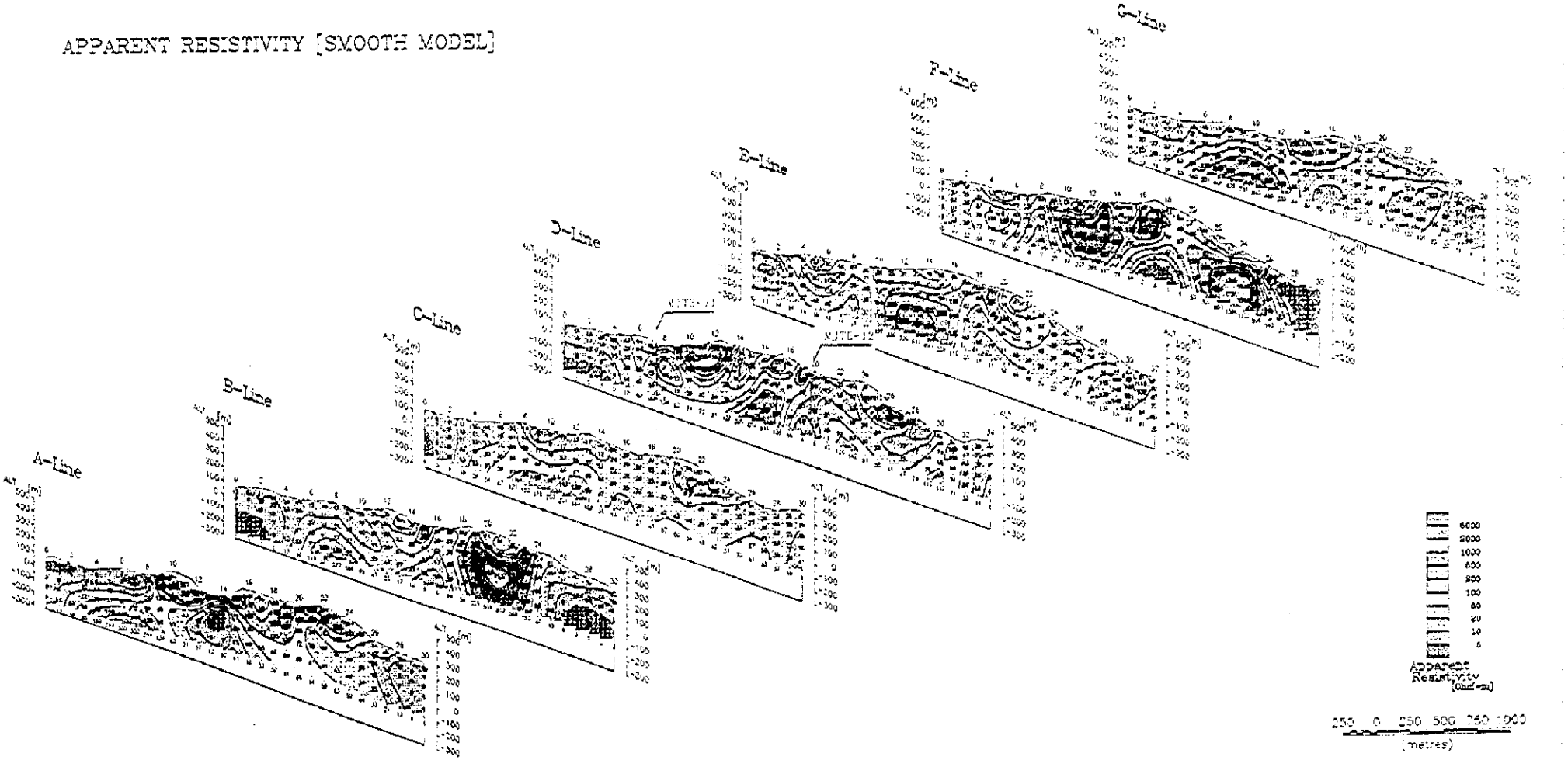

Fig.II-3-27 IP Sections of Simulated Result in Karılar Area (Resistivity)

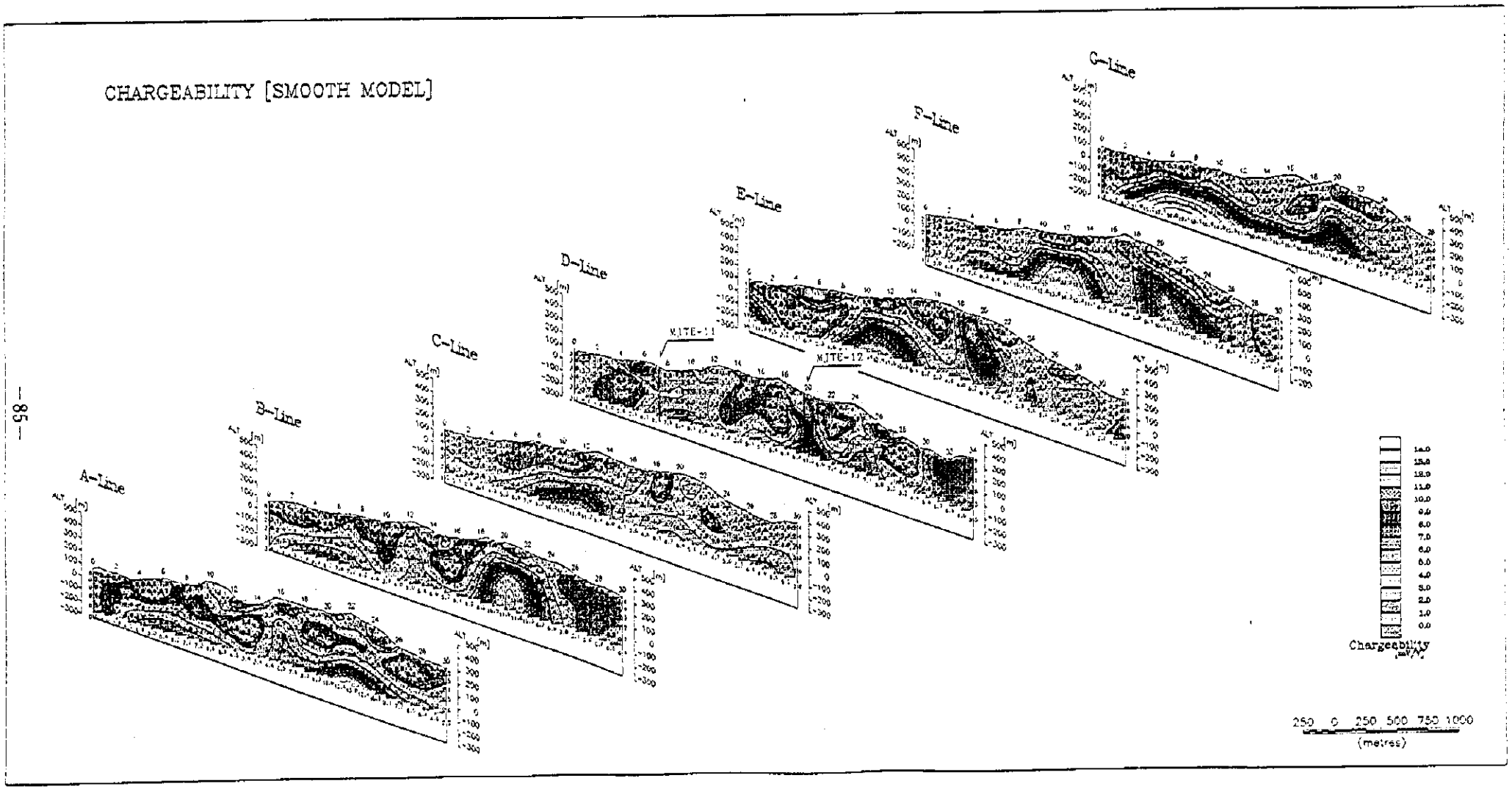

Fig.II-3-28 IP Sections of Simulated Result in Karılar Area (Chargeability)

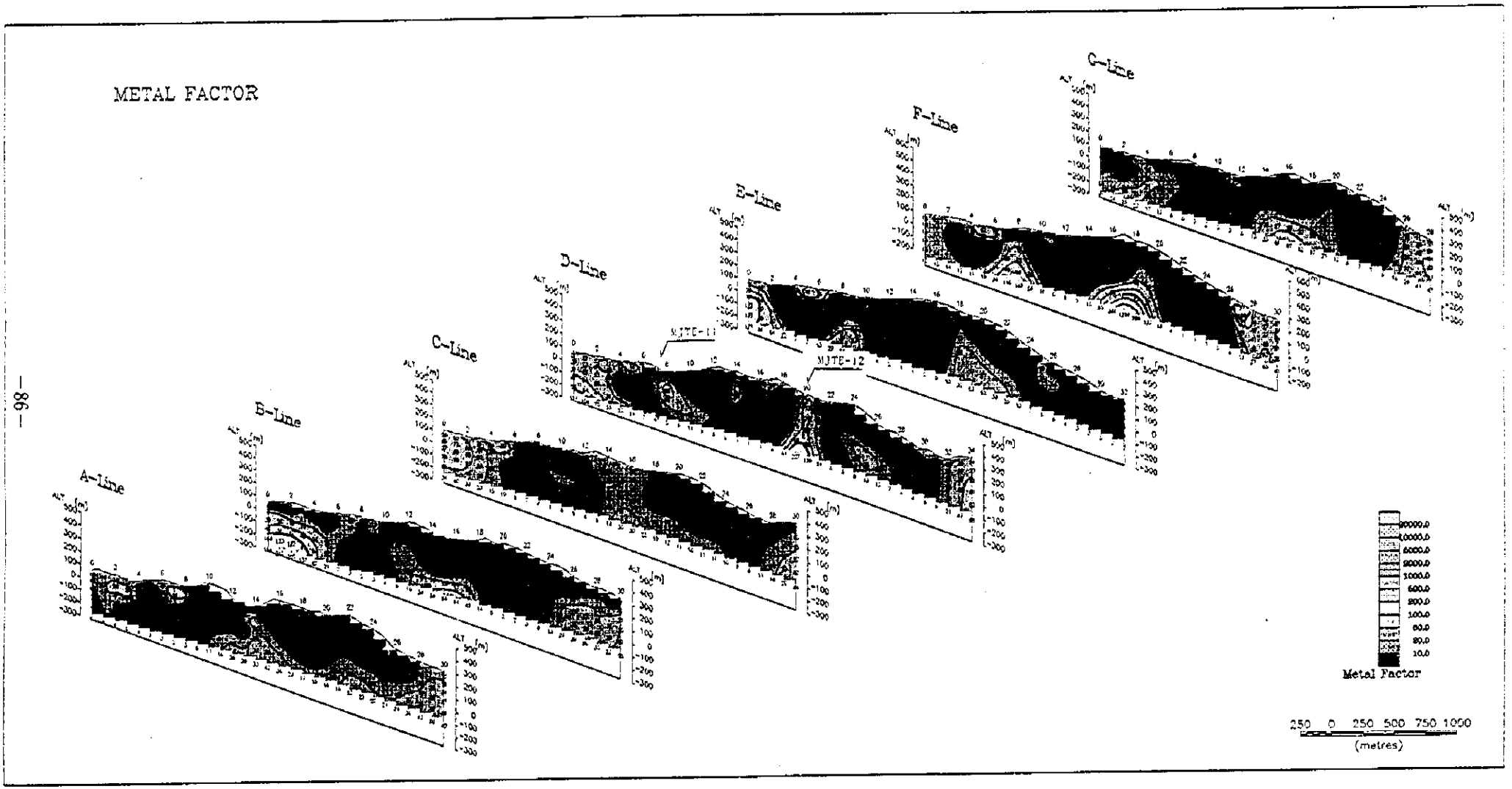

Fig.II-3-29 IP Sections of Simulated Result in Karılar Area (MF)

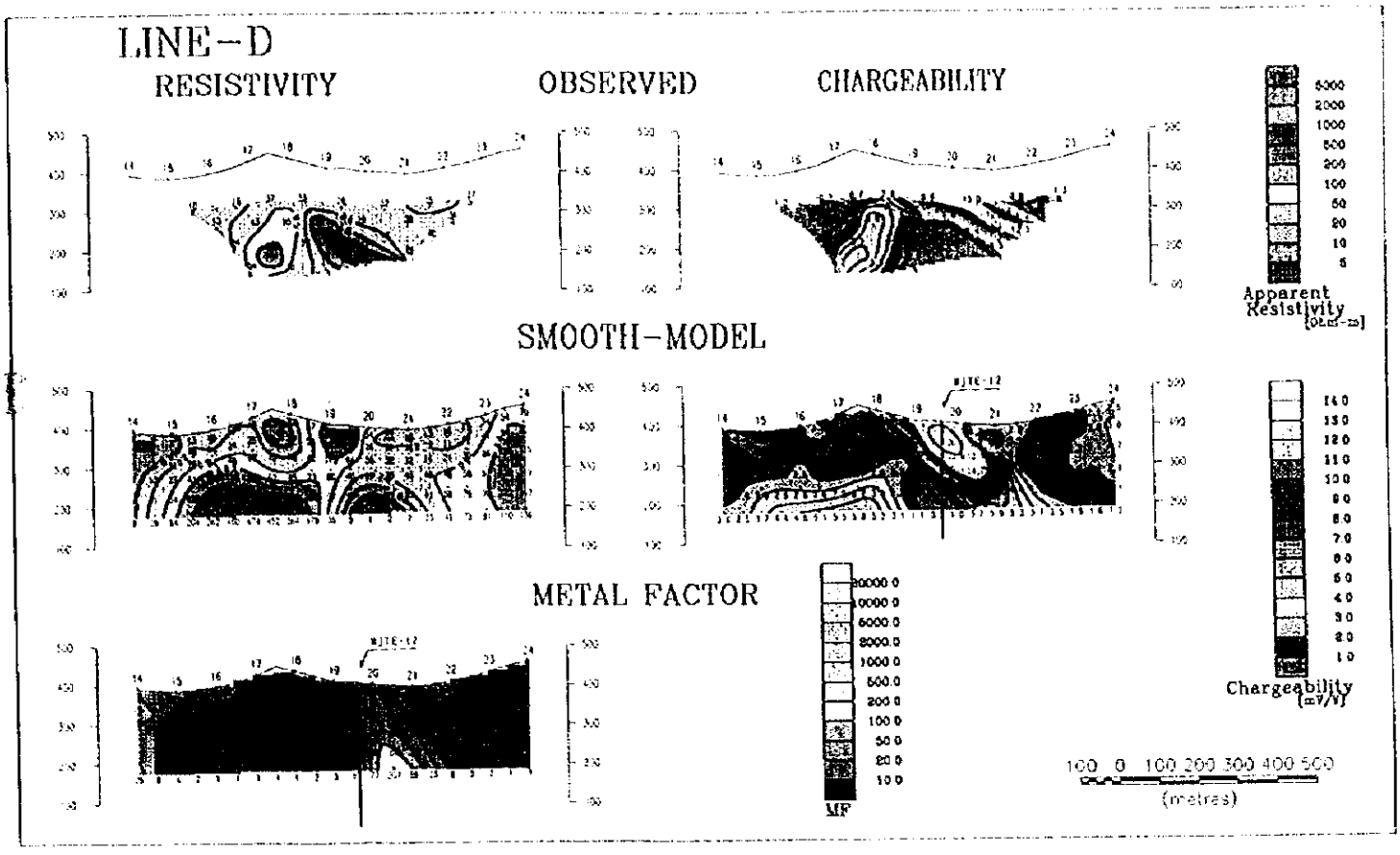

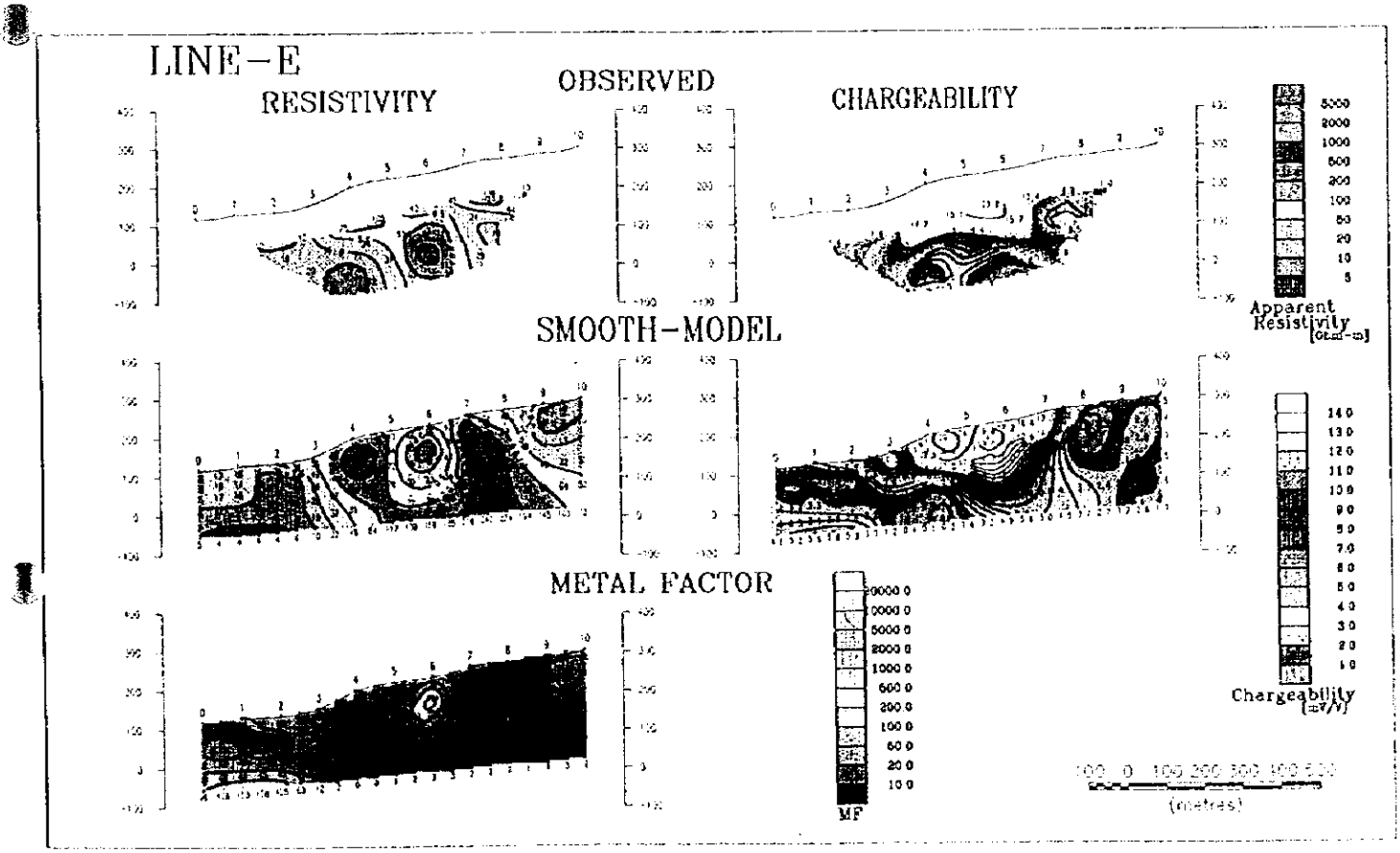

Fig.II-3-30 IP Sections of Simulated Result in Karılar Area (a=100m)

2.CSAMT Method

(1) Results of the Survey

The results of the survey are shown in Table II-3-31.

Within the range of high to medium frequencies, low resistivity zone of about 30 Ω·m or less is predominant.

Site No.23 of Karaerik deposit and site No.8 near Karılar deposit belong to a small-scale high resistivity zone.

A low resistivity zone extends from northwest of the surveyed area to approximately the central part of Topuklu Tepe, located in SE direction.

(2) Results of Analysis

Results of the analysis are shown in Fig. II-3-32~35.

Section of 1-D Resistivity Structure (Fig.II-3-32)

Broadly studying all the sections, it can be considered that, in general, the resistivity structure of this area was analyzed as 2 or 3 layered structure, and the resistivity at deep level is high and can be estimated to be about 150 Ω·m or more.

The resistivity structure at the depth of site No.23 of Karaerik deposit and that at the depth of site No. 8 of Karılar deposit exhibit relatively high value such as about 200 Ω·m or more.

Plane Map of 1-D Resistivity Structure (Fig.II-3-33)

In general, the low resistivity zone of 50 Ω·m or less distributes widely reaching near the depth of about 200m. Further, judging from the overall distribution of resistivity, it can be considered that the E-W-trending low resistivity structure is existing mainly in the vicinity of Karılar ore deposit.

Section of 2-D Resistivity Structure (Fig.II-3-34)

The resistivity structure sections of the lines a, b and c are made up into a panel diagram.

In general, the resistivity structures are analyzed into 3 layered structure comprising layers of 100 Ω·m or more, 100-50 Ω·m and 50 Ω·m or less.

The resistivity structure of 100 Ω·m or more at a deep level was considered to dipping toward in a northwestern direction.

(3) Consideration

The results of analyses by IP method and CSAMT method are summarized into a comprehensive analytical map (Fig.II-3-35).

The apparent resistivity in the surveyed area varies from several Ω·m to 600 Ω·m. The zone covered with hematite dacite shows usually high resistivity (100 Ω·m or more in general), in this area however, its vlues are ranging from several Ω·m to 600 Ω·m. In the hematite dacite distribution area, especially, in a low resistivity zone of several Ω·m, the intense argillization was observed on the surface, indicating that the presence of the fractures and argillization are major factor causing the variation of the resistivity.

In general, the resistivity of other rocks is as low as about 50 Ω·m or less, mainly caused by the argillic alteration.

According to the results of measurement, the apparent resistivity was within the range of several Ω·m-600 Ω·m, whereas according to the results of Inversion analysis, the calculated resistivity was within the range of several Ω·m-about 1,600 Ω·m. A high resistivity zone of about 1,000 Ω·m or more was analyzed to exist at the depth of 50m or more. Further, according to the result of analysis, in the hematite dacite distribution area, a slightly high chargeability was observed corresponding to the high resistivity zone, this tendency, however being observed throughout the results of the analyses of all the samples.

According to the results of IP survey, the values of chargeability were found to be low in general. Near the Karaerik and Karılar deposits, the weak but obvious anomaly zones were found.

The weak anomaly zones of MF were identified in site No.8 in the line D and near the site No. 29 the line F.

Near the Karaerik and Karılar deposit the distribution form of mineralization was clarified through the measurement by the electrode spacing of 100m.

According to those values of MF as determined by analysis, when the unit described above was adopted, the value of MF was found to be 100 at a maximum near the old ore deposit. Further, the largest value of MF within the surveyed area was 200 as observed near the site No. 27 in the line F. However, according to the results of the property tests of ore samples in terms of the relationship between the value of MF and the mineralization, the value of MF was about 10 or less where there was no mineralization, about 100-1,000 for siliceous ore, about 2,000 or more for black ore and about 10,000 or more for yellow ore. Judging from these facts, it can be considered that the presence of a weak anomaly of MF suggests the presence of weak mineralization.

According to the results of the resistivity analysis by IP method and the result of 1D analysis by SCAMT method, it can be identified that the low resistivity structure running east-west direction exists at about the center and north of the surveyed area.

Concerning the results of the analysis by the CSAMT method, the distribution of resistivity in neighboring regions are not clear because of insufficient number of measuring points; however, the results of analysis indicate that near the Karaerik deposit and the Karılar deposit, slightly high resistivity was observed even in relatively deep level.

According to the result of 2-dimensional analysis, high resistivity (100 Ω·m or more) was observed in general at deep levels. The depth of region exhibiting high resistivity is estimated to be about 300-600m, this region being considered gently inclining downward in the northwestern direction of the surveyed area. This tendency coincides with the result of gravity structure.

3-2-4 Summary

The low resistivity zones detected by IP and CSAMT survey reflect the alterration zones in general. Espesically low resistivity zone of several Ω·m corresponded to intense argllization zone.

Low resistivity structure of E-W trending was indentified in the Karılar area. It is considered that this stracture might be related with the mineralization in this area.

High resistivity zone of 300 Ω·m or more coresponded to the intrusive rocks well.

Some anomaly zones of chargeability were fond near ore horizone in Taflancık and Kalıral area. But the results of analysis showed the possibility of weak mineralization only.

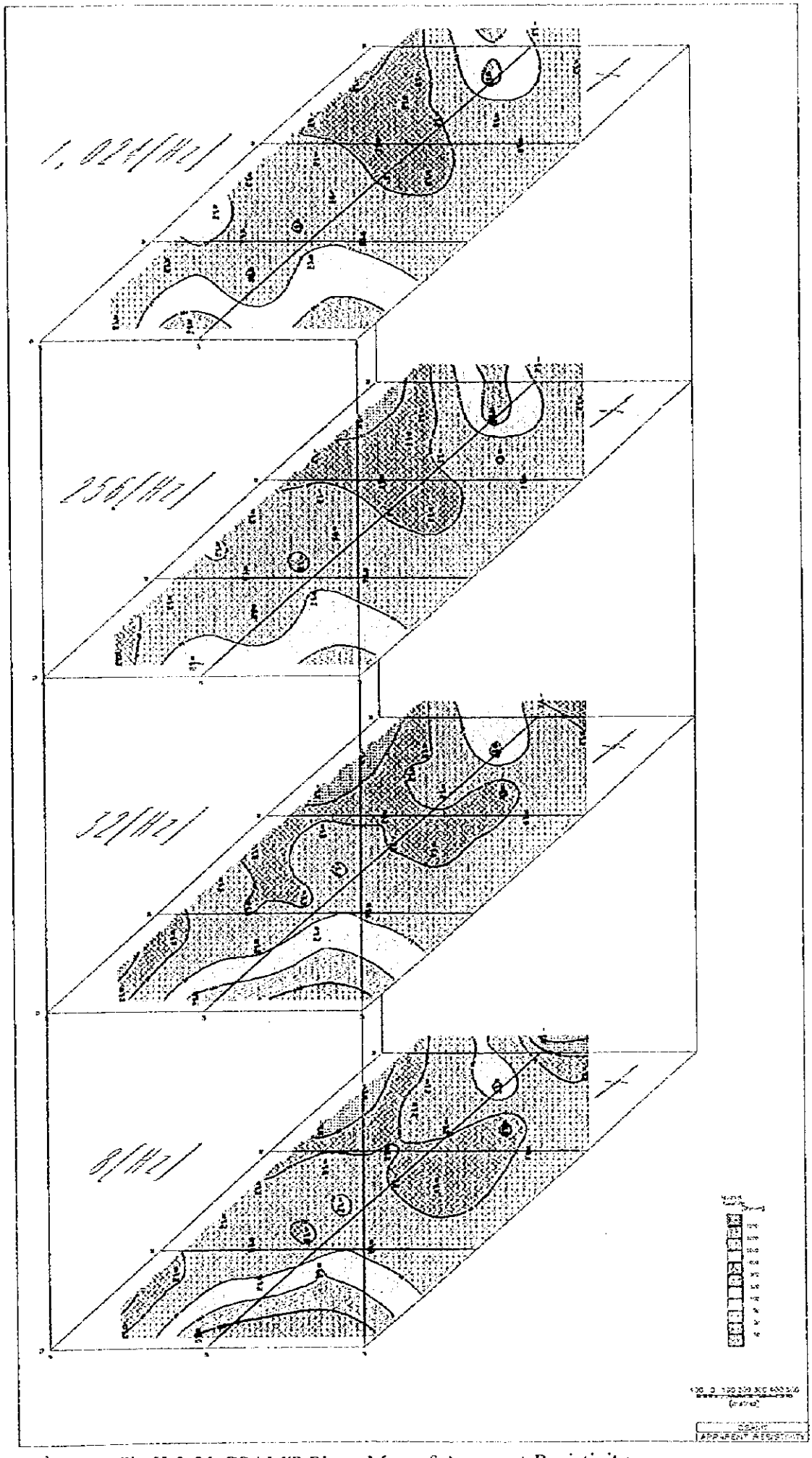

Fig.II-3-31 CSAMT Plane Map of Apparent Resistivity

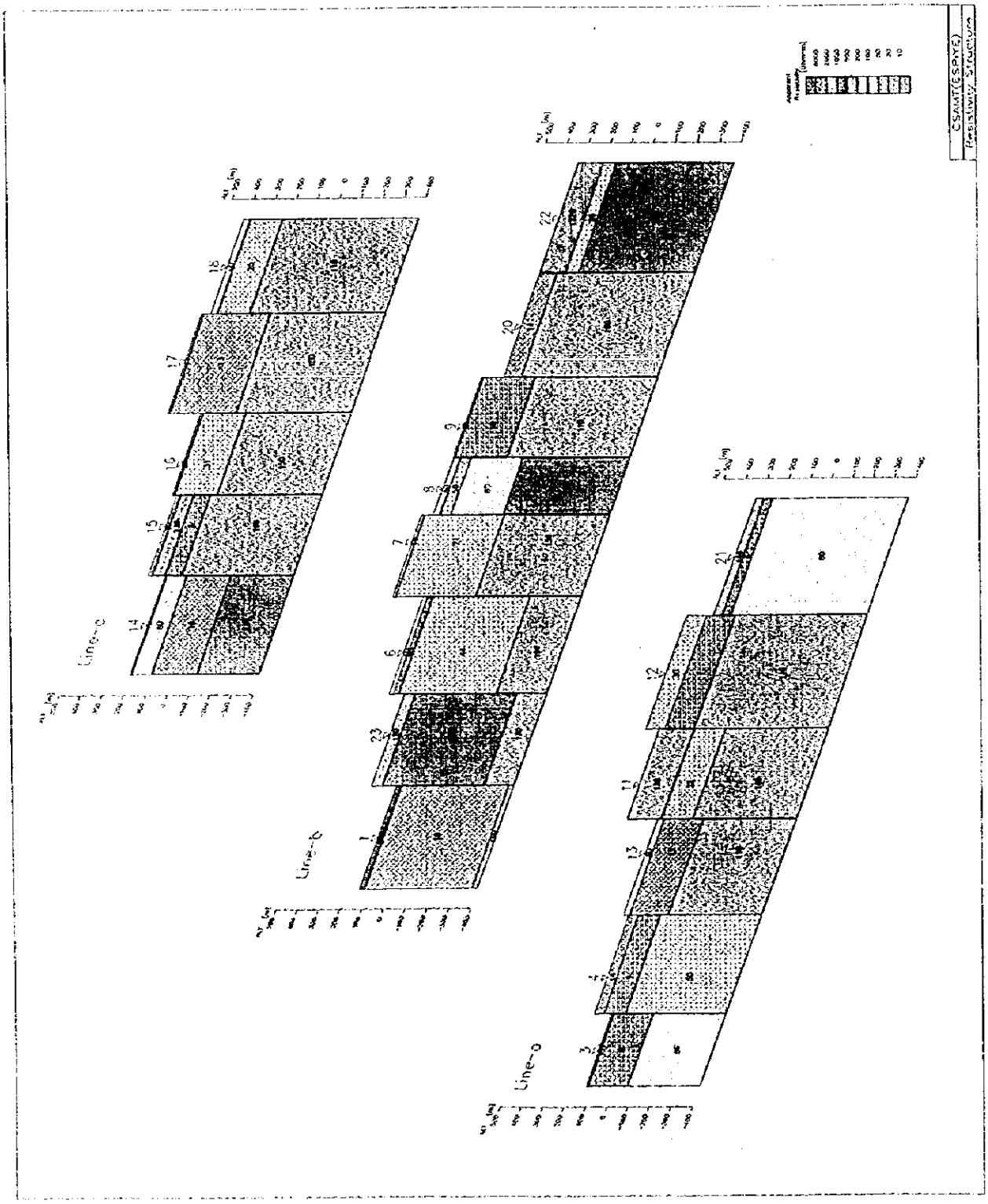

Fig.II-3-32 CSAMT 1D Section of Resistivity Structure

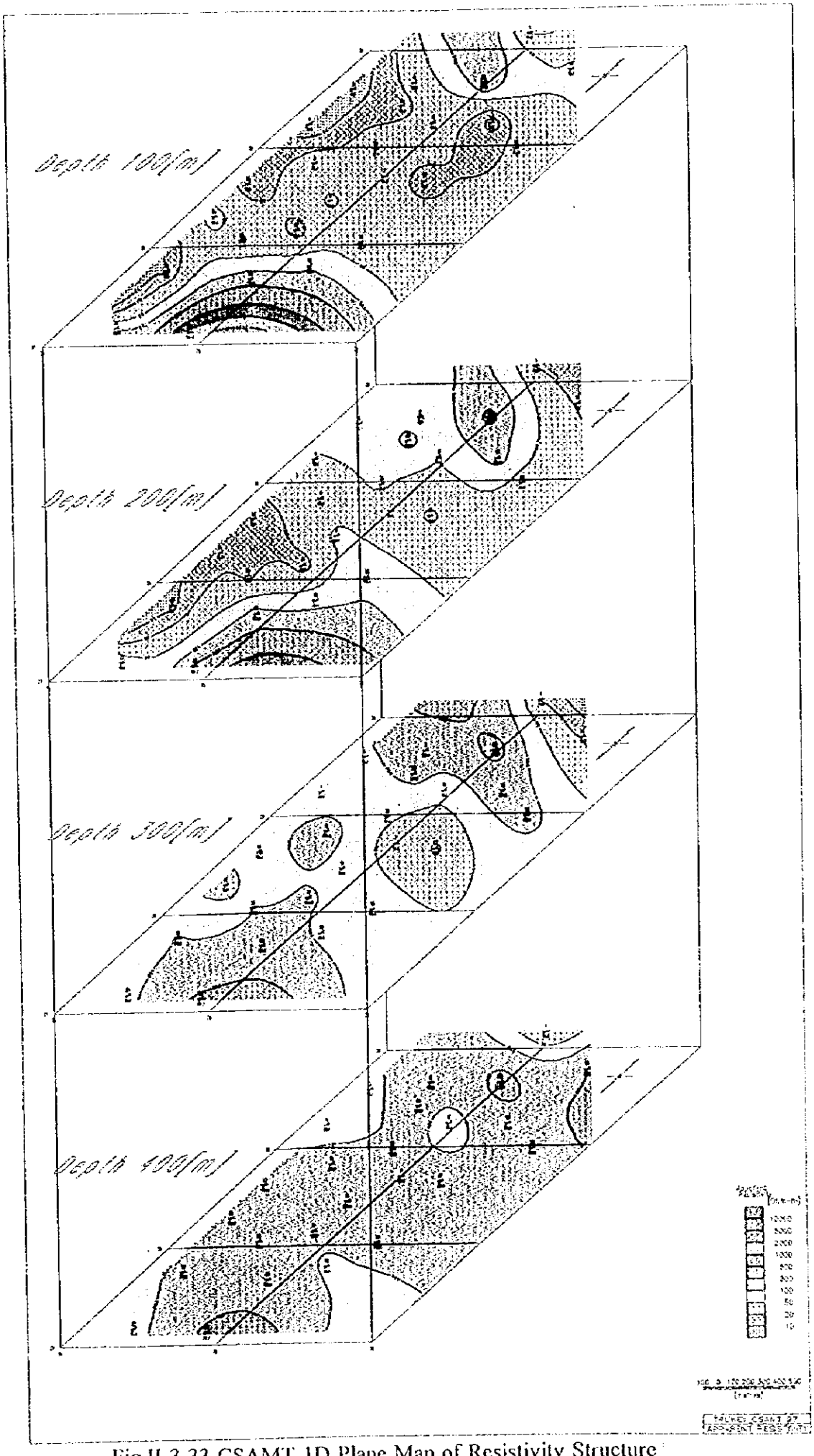

Fig.II-3-33 CSAMT 1D Plane Map of Resistivity Structure

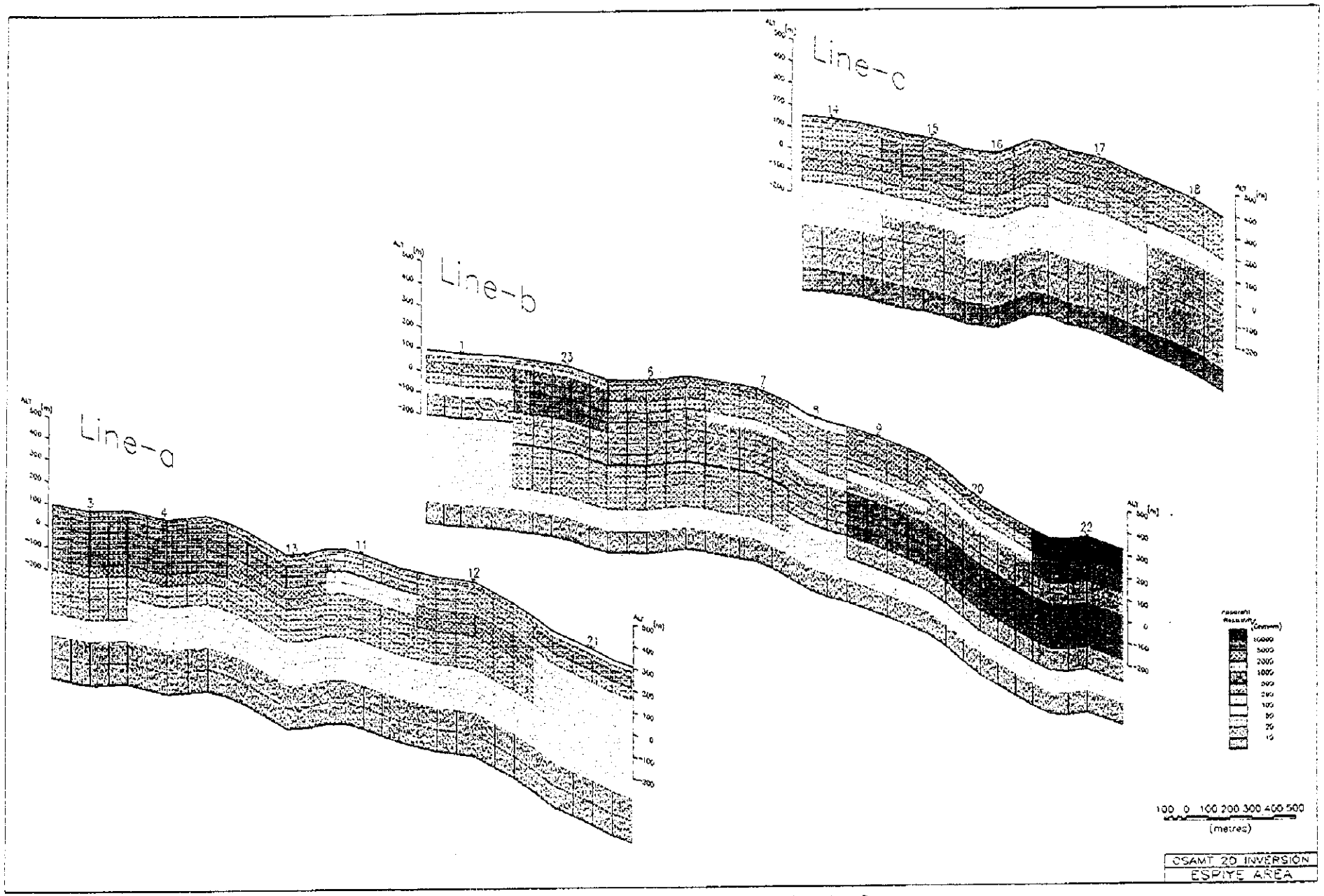

Fig.II-3-34 CSAMT 2D Section of Resistivity Structure

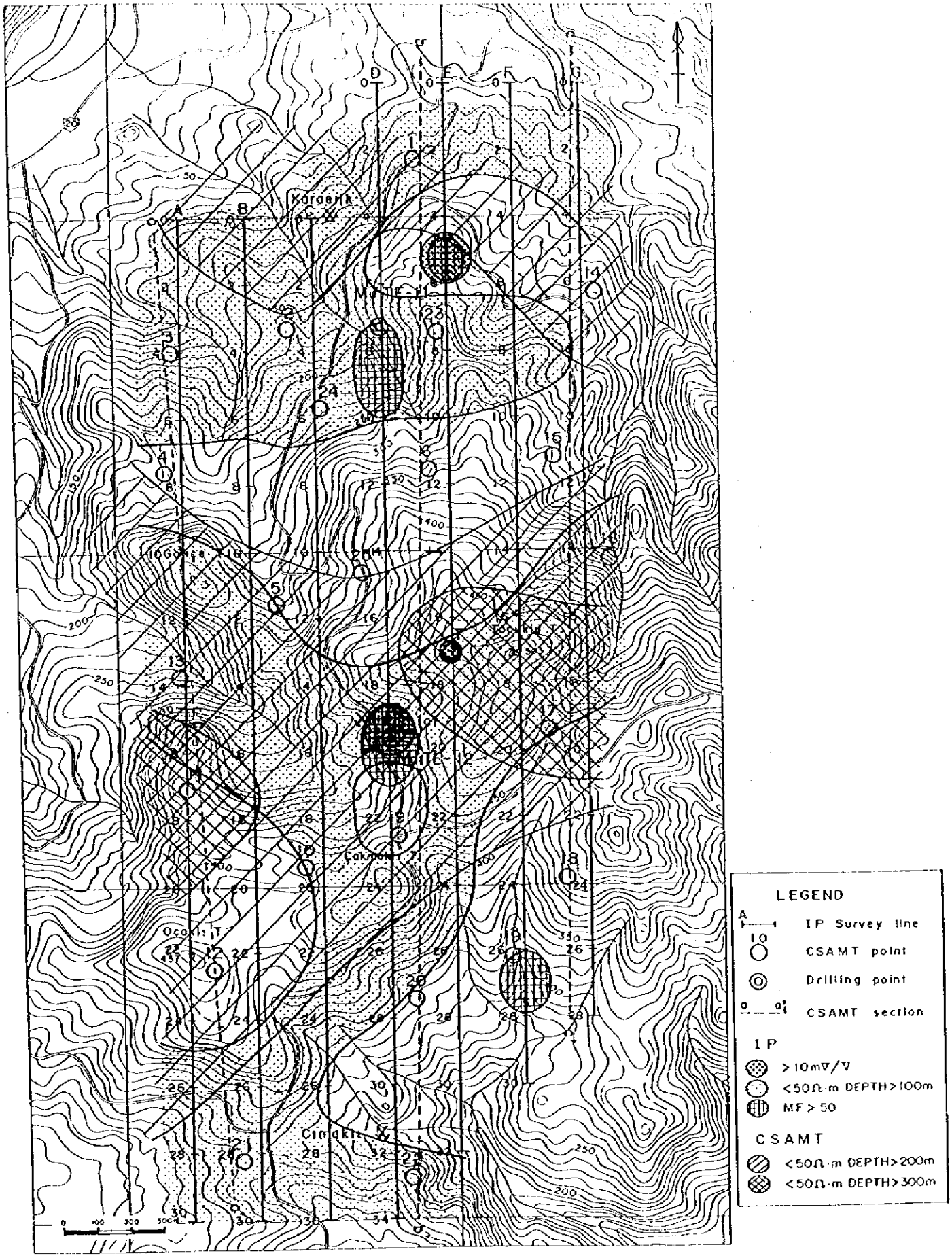

Fig.II-3-35 Summarized Map of IP and CSAMT Method in Karılar Area

Chapter 4 Drilling Survey

4-1 Survey Method and Survey Content

Drilling survey was carried out at 12 sites(see Fig. II-4-1 and Fig II-4-2) in the promising area selected by geological survey, geophysical survey etc., in order to investigate the mineralization, ore horizon and geological structure. Details of the survey and survey results are described below.

Area	Drilling No.	Depth	Inclination
Killik	MJTE-1	250m	-90
Kepcerik	MJTE-2	260m	-90
Bitene	MJTE-3	150m	-90
	MJTE-4	212m	-90
	MJTE-5	261m	-90
Taflancık	MJTE-6	200m	-90
	MJTE-7	200m	-90
	MJTE-8	200m	-90
	MJTE-9	250m	-90
	MJTE-10	250m	-90
Karılar	MJTE-11	400m	-90
	MJTE-12	350m	-90

4-2 Results of the Survey

Geological sections are shown in Fig.II-4-3~II-4-7, and results of the chemical analysis are shown in Table II-4-1.

MJTE-1

The drilling site is located at the point 1.25Km ESE from Killik deposit. This point is midst point of Killik deposit and Kızılkaya deposit. Hematite dacite covers around drilling point and IP anomaly is found in deep part of this point. Mineralized outcrop is observed in its southern stream.

Relatively thick hematite dacite is intersected from surface to the depth of 170m and lower than that, dacite of the Kızılkaya Formation continues down to the bottom accompanying thin aphyric dacite of the Çağlayan Formation between those Formations. Autobrecciated structure and plagioclase phenocryst are found in the dacite of the Kızılkaya Formation.

Aphyric dacite of Çağlayan Formation and dacite of the Kızılkaya Formation have undergone intense sericitization with partial silicification.

Dissemination zone(25cm) of chalcopyrite (Cu 4.88%) is observed at 234m depth as well as sporadic and intense dissemination and stockwork of pyrite occur at more than 170m in depth, but its grade is rather low.

As the results, it is revealed that the IP anomaly is reflected the alteration and mineralization zone at more than 170m in depth. And the IP anomaly zone of foodwall dacite defined in the south of

drilling point possibly indicates the stockwork mineralization of sulfides.

MJTE-2

The drilling site is located at a point close to ridge some 500m south of Kepçelik prospect. The drilling hole is located midst point of the old Kepçelik pit and mineralized outcrop at east of the drilling point, and weak IP anomaly is recognized in deep part.

A series of dacitic volcanics of the Çağlayan Formation such as tuff, lapilli tuff, tuffbreccia, aqueous autobrecciated lava, lava dome of aphyric dacite, has been intersected from surface to 206m in depth. The lower unit than this stratum consist of autobrecciated dacite of the Kızılkaya Formation, andesitic pyroclastics of the Çatak Formation and plagioporphyritic dacite intrusive.

As for alteration, weak chloritization and sericitization were observed in the Çağlayan Formation. The Kızılkaya Formation has undergone general alteration mainly of quartz, sericite and pyrite. The Çatak Formation shows intense skarn-like alteration of intensive chloritization, epidotization and calsitization is observed. The intrusive rocks at the undermost part is affected by chlorite and sericite.

The weak mineralization of stockwork~vein of sulfides is observed in the Kızılkaya Formation, of which grade is at the level of Cu 0.20%, Pb 0.74%, Zn 0.94%. Thin vein of chalcopyrite- sphalerite occurred in the Çatak Formation.

From those results and existing data, it has been considered that there is a little possibility of existence of significant scale of ore body in the vicinity of Kepçelik area.

MJTE-3

The drilling site is located at the ridge, 750m northeast from north Killik deposit. Some floats of massive sulfides were found at the stream in NNW direction to the drilling point.

A series of dacitic lapilli tuff, tuff, sandy tuff and those alternations of the Çağlayan Formation was observed from surface to 78.9m in depth, The tuff substantially contains greenish volcanic glass. Dip of the bedding plane shows 10 to 15°. Thin layers of pyrite and ferruginous chert are intercalated to fine sandy tuff as the base and they have particular characteristics of hanging wall. The unit lower than 78.9m is autobrecciated dacite of the Kızılkaya Formation consisting phenocryst of quartz and plagioclase. Additionally, small scale dikes of quartz porphyry and aphyric dacite are observed.

Weak argillization mainly of sericite and chlorite is observed in the Çağlayan Formation but partially intense argillization mainly of quartz and sericite is observed in the Kızılkayan Formation.

Intense stockwork mineralized zone mainly consisting of pyrite is intersected in 108.9 to 115m depth of Kızılkaya Formation, accompanied by massive yellow ore of 20cm thick (Au 2.06ppm, Ag 15.3ppm, Cu 12.58%, Pb 0.04%, Zn 0.02%, Fe 24.58% and S 27.67%) at its upper most part.

MJTE-4

The drilling site is located at a point 500m north from Killik deposit where weak IP anomaly is spreading.

A series of dacitic volcanics of the Çağlayan Formation such as lapilli tuff or tuff, stratified fine

tuff, sandy tuff and those alternations is intersected from the surface to the depth of 133.4m. In the same manner as the MJTE-3, the tuff is accompanied by greenish volcanic glass. Geology from 139.85m in depth to the hole bottom is autobrecciated dacite lava of the Kızılkaya Formation and it is recognized that plagioclase phenocryst remains there. Andesite dikes intrusing the Çağlayan and Kızılkaya Formations are recognized very often. This intrusive is of the same characteristic one as distributed over Killik Tepe north to the drilling point.

As for alteration, sericitization (argillization) is predominant except andesite dikes, and chlorite or scarcely gypsum are accompanied in the Çağlayan Formation. The dikes is affected by alteration of chlorite and calcite.

As for mineralization, stockwork - vein of pyrite is partially predominant but, on the whole, the size is rather small and grade is low.

MJTE-5

The drilling site is located at around 500m south from Lahonos deposit. Altered aphyric dacite of the Çağlayan Formation distributes around surface of the drilling point where is included in weak IP anomaly zone.

Aphyric dacite lava of the Çağlayan Formation has been observed from surface to 130.7m in depth and underlain by autobrecciated dacite lava of the Kızılkaya Formation sometimes accompanied by essential fragment including abundant plagioclase phenocrysts. Other than that, hematite dacite (porphyritic) intrusive and andesite dikes are observed.

Argillic alteration of sericite occurs in the Çağlayan Formation, accompanying kaolinite, and also alteration of quartz and selicite (partially kaolinite) in the Kızılkaya Formation is observed and small amount of chlorite appears in deeper part.

Some small veins of sulfides are found even in the Çağlayan Formation and relatively intense stockwork of pyrite occurs in the Kızılkaya Formation. Dissemination of fine pyrite is observed in argillized part between the Çağlayan Formation and Kızılkaya Formation, and the result of chemical analysis shows rather high grade of Au 0.35ppm, Ag 7.50ppm, Cu 2.18%, Zn 0.02%, Fe 10.46% and S 11.65%.

MJTE-6

The drilling site is located at northeast end of wide IP anomaly zone, where hematite dacite distributes in surface area. Alteration zone accompanying mineralization distributes in stream at north of the drilling site.

Hematite dacite has been observed from surface to 72.3m in depth and underlain by the Kızılkaya Formation in deeper part which consists of poor phenocryst dacite lave, dacitic tuff, autobrecciated dacite lava rich in plagioclase phenocryst and dacitic tuff breccia (more than 160m in depth).

Intense alteration with chlorite and sericite appears in the Kızılkaya Formation but chloritization becomes predominant at tuff breccia in the lower part.

As for mineralization, some fragments of yellow ore (5cm in the maximum radius) and plenty of mineralized fragments are found in the Kızılkaya Formation directly underlay the hematite dacite. At the Kızılkaya Formation in lower part, coarse pyrite dissemination and partially intense stockwork mineralization are observed, occasionally accompanied by chalcopyrite.

From the fact that yellow ore was found, existence of the background (supply source) was presumed around this part.

MJTE-7

The drilling site is located at southern end of wide IP anomaly zone and mineralized outcrop is observed along the Örendere stream in the south.

Aphyric dacite of the Çağlayan Formation from surface to 145.5m in depth accompanied by thin layer of lapilli tuff. Dacite lava and tuff breccia of the Kızılkaya Formation, containing plagioclase phenocryst with intense autobrecciation structure, are observed at the part deeper than this.

Alteration in the Çağlayan Formation is weak argillization accompanied by chlorite-sericite, but intense argillization accompanied by sericite, kaolinite, magnesite and pyrite without chlorite occurs in the Kızılkaya Formation.

Some pyrite veinlets are found in the Çağlayan Formation and intense dissemination - stockwork of pyrite in the Kızılkaya Formation is observed, which is partially accompanied by fine vein of chalcopyrite.

MJTE-8

The drilling site is located at central east part of wide IP anomaly zone.

Hematite dacite with partial brecciation and flow banding appears from surface to 104.5m in depth. Also, the geology at the part deeper than 104.5m is the Kızılkaya Formation consisting of dacite lava, tuff and tuff breccia. There are a few varieties of lava such as aphyric lava, porphyritic lava and brecciated lava.

Hematite dacite has undergone weak argillization with trace of chlorite and sericite. In the Kızılkaya Formation, argillization mainly of sericite is predominant and, in tuff breccia at deep part, chlorite is tend to increase.

Some dissemination and stringer of pyrite are partially developed in the Kızılkaya Formation but the grade is not so high. Mineralized clay vein filled with shear zone occurs in hematite dacite, the grade shows comparatively high (Zn 1.50%).

MJTE-9

The drilling site is located at northern end of wide IP anomaly zone.

Hematite dacite occurs from surface to 113.8m in depth and underlain by the Kızılkaya Formation consisting mainly of dacitic tuffs rich in greenish volcanic glass and gradually change

into lava. Both tuffs and lava contain coarse phenocryst of plagioclase. At the deeper part, tuff breccia in green color is found and is rich in accessory dacitic fragments and porphyritic dacite rock intruded in the Kızılkaya Formation at 2 points.

Hematite dacite and porphyritic dacite are affected by weak calcitization. The alteration in the Kızılkaya Formation is weak in comparison with the Kızılkaya Formation in other drilling holes and shows mainly of weak argillization accompanied by a few amount of sericite, chlorite but strong chloritization occurs in tuff breccia at deeper part.

Mineralization is rather weak on the whole, and pyrites films is found at the points close to 138m in depth and a few fine veins of Cu-Pb-Zn occurs in tuff breccia at deep part.

MJTE-10

The drilling site is located at almost center point of wide IP anomaly zone.

The borehole geology consists, from surface, of hematite dacite, aphyric dacite of the Çağlayan Formation, dacite intrusive rock and the Kızılkaya Formation. The hematite dacite and dacite intrusive rock have well developed joint structure. The Çağlayan Formation shows aphyric and partial breccia structure. The Kızılkaya Formation consists mainly of plagioclase porphyritic massive lava, autobrecciated lava and deep green colored tuff breccia appears in deeper part.

Alteration is observed even in hematite dacite in shallow part and the dacite is decolored accompanied by montmorillonite and calcite veins. The Çağlayan Formation is affected by weak argillization mainly of sericite and dacite intrusive is decolored along fracture. In the Kızılkaya Formation, argillization is more apparent at lava part accompanying sericite, chlorite and pyrite but intense chloritization is dominant in tuff breccia in deep part, accompanying small amount of calcite and pyrite.

Mineralization is found mainly in lava of the Kızılkaya Formation with extent of existence of weak partial network of fine pyrite veins and not of high grade.

MJTE-11

The drilling site is located at the south of the Karaerik deposit and in alteration zone continuing from the Karaerik deposit. Weak IP anomaly was found at deep part of the drilling point.

The borehole geology consists of dacitic tuff and lava, rhyolite of the Çağlayan Formation, quartz-plagioclase porphyritic intrusive. The Çağlayan Formation distributing down to 90m in depth has undergone intense alteration and original lithology could not identified, but, at the deeper zone, original texture of aphyric, flow banding and breccia-autobreccia was observed. The rhyolite shows perlitic and brittle feature on the whole, composed of coarse quartz, plagioclase and fresh hornblende. Porphyritic intrusive rock has hard and magnetic property, and contains a plenty of phenocrysts of quartz and plagioclase. Chilled margin of this intrusive was observed in boundary

zone.

Argillic alteration is traced down to around 205m in depth and, especially down to 90m in depth, intense argillization mainly of sericite, kaolinite and pyrite without chlorite is observed, but at more deeper zone, alteration mainly of sericite and chlorite is predominant. Sericite-montmorillonite intermixed layers and mordenite occurred in the rhyolite but the alteration is categorized as weak diagenesis. The intrusive rock is affected by intense argillization at shallow part and the alteration is gradually weakened with increment of depth.

Mineralization is limited in argillized zone at part down to around 200m in depth, and no mineralization is observed at part deeper than this. Dissemination of pyrite is intense at shallow part, accompanied by fine veins of chalcopyrite but the maximum grade is Cu 0.17%. At the depth of around 200m, fine veins accompanying chalcopyrite and sphalerite are well developed in intrusive rocks, and the grade is Cu 0.20% and Zn 1.46%.

Since mineralization gradually decrease in the intrusive rocks and no more mineralization is observed in the deeper zone, Karearik deposit is considered to be a stockwork type deposit formed later than the Lahanos type.

MJTE-12

The drilling site is located at the south from Karılar deposit, where IP anomaly continues down to deep level.

The borehole geology consists of breccia of hematite dacite, plagioclase porphyritic dacite, porphyritic dacite of the Çağlayan Formation, dacitic tuff, rhyolite, alternation of tuff and basalt, basaltic andesite and dacitic hydrolcastite of the Çağlayan Formation and dacite lava of the Kızılkaya Formation. Quartz porphyritic dacite intruded in both Çağlayan and Kızılkaya Formations. The rocks at the point deeper than 260.4m are considered to be water laid origin.

The intense argillization mainly of sericite, kaolinite and pyrite has occurred from surface to 223.4m in depth, accompanied by carbonate minerals. In the area deeper than 223.4m, the alteration extremely decrease to a level of weak argillization, but sericite and montmorillonite mixed layer minerals appear with increment of depth, and the dacite of the Kızılkaya Formation is affected by trace of sericite and chlorite.

Mineralizaiton is limited within intense argillization zone mainly in shallow part, which consists of dissemination and stockwork of coarse pyrite. Massive (pyrite) part of 70cm thick is observed but it's grade shows low value except Fe. In the argillized porphyritic dacite of the Çağlayan Formation, sphalerite and chalcopyrite are visibly recognized and the grade is rather high compared to the other parts (Au 1.63ppm, Ag 9.77ppm, Zn 1.39%). Also, fine veins of pyrite are observed in dacite of the Kızılkaya Formation but the grade of each consisting element is low.

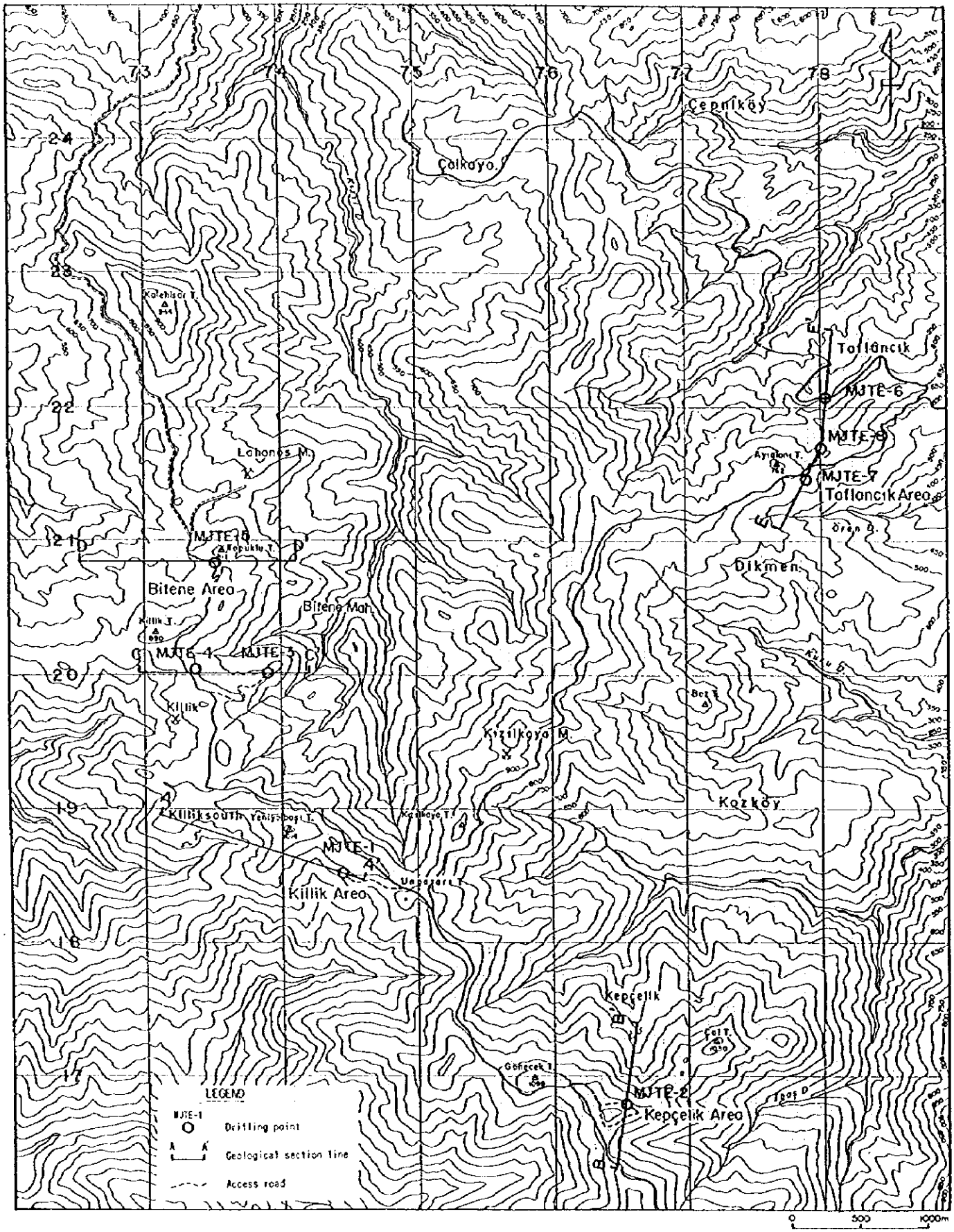

Fig.II-4-1 Location Map of the Drilling Sites (Bitene~Taflancık Area)

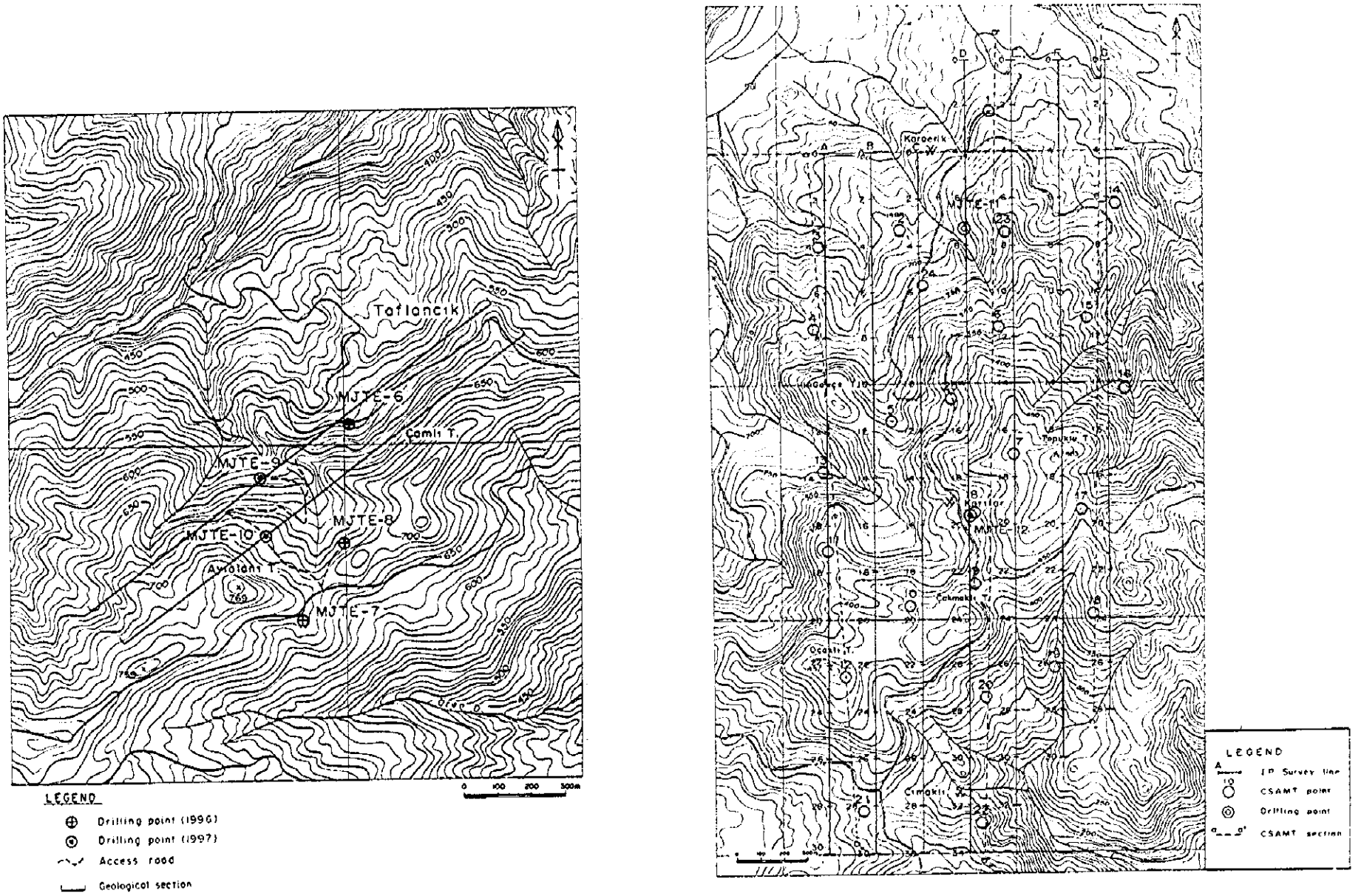

Fig.II-4-2 Location Map of the Drilling Sites (Taflancık and Karılar Area)

Table II-4-1 Results of the Chemical Analysis of Core Samples (1)

NO.	DRILLING NO	DEPTH (m)	SAMPLE TYPE	AU (ppm)	AG (ppm)	CU (%)	PB (%)	ZN (%)	FE (%)	S (%)	REMARKS
A-1	MJTE-1	180.0-180.5	sil pyrite diss	0.02	0.74	< 0.01	< 0.01	0.03	12.67	14.49	
A-2	MJTE-1	182.0-182.2	arg pyrite diss	< 0.01	1.14	< 0.01	0.03	0.09	12.77	14.69	
A-3	MJTE-1	202.7-202.9	sil pyrite diss	< 0.01	0.15	< 0.01	< 0.01	< 0.01	9.50	10.84	
A-4	MJTE-1	221.0-221.2	sil pyrite net	0.03	0.10	< 0.01	< 0.01	< 0.01	4.42	5.12	
A-5	MJTE-1	226.7-227.2	sil pyrite net	0.02	0.15	< 0.01	< 0.01	< 0.01	7.87	9.08	
A-6	MJTE-1	234.5-234.65	chalcopyrite diss	< 0.01	3.11	4.88	< 0.01	< 0.01	16.61	18.61	
A-7	MJTE-1	250.0-250.50	pyrite diss ore	< 0.01	< 0.01	< 0.01	< 0.01	< 0.01	6.43	7.13	
A-8	MJTE-2	207.0-207.5	pyrite diss	0.14	3.75	0.20	0.74	0.94	3.26	4.14	cp. bearing
A-9	MJTE-2	210.3-210.8	pyrite diss	0.05	0.15	< 0.01	< 0.01	0.01	1.92	1.88	
A-10	MJTE-2	215.0-215.5	pyrite diss	0.08	0.35	0.05	0.08	0.52	2.30	2.72	cp. film
A-11	MJTE-2	220.0-220.5	pyrite diss	0.05	0.15	< 0.01	< 0.01	< 0.01	2.21	2.56	
A-12	MJTE-2	240.7-240.8	sph+cp+py vein	0.06	1.87	0.31	0.01	8.15	5.18	9.00	
A-13	MJTE-3	76.5-76.6	py. band tuff	0.04	< 0.01	< 0.01	< 0.01	< 0.01	24.00	23.64	
A-14	MJTE-3	109.05-109.20	yellow ore	2.06	15.30	12.58	0.04	0.02	24.58	27.67	
A-15	MJTE-3	114.8-114.9	pyrite network	0.04	0.20	0.02	< 0.01	< 0.01	37.92	42.38	
A-16	MJTE-3	116.0-116.2	pyrite diss	0.20	1.28	< 0.01	< 0.01	< 0.01	20.35	23.33	
A-17	MJTE-3	130.7-130.8	powder pyrite net	0.26	0.34	< 0.01	< 0.01	0.03	24.77	27.33	
A-18	MJTE-3	133.85-133.9	pyrite network	0.40	1.23	< 0.01	< 0.01	0.01	22.85	25.62	
A-19	MJTE-3	145.1-145.2	pyrite diss	0.06	0.05	< 0.01	< 0.01	< 0.01	15.74	5.07	
A-20	MJTE-4	177.5-177.6	pyrite diss	0.08	< 0.01	< 0.01	< 0.01	0.02	2.69	2.76	
A-21	MJTE-4	199.7-199.8	pyrite diss	< 0.01	0.25	< 0.01	< 0.01	< 0.01	5.95	7.02	
A-22	MJTE-4	211.3-211.5	powder pyrite net	< 0.01	0.10	< 0.01	< 0.01	< 0.01	20.93	24.14	
A-23	MJTE-5	61.2-61.3	hm+py+cp vein	0.09	0.69	< 0.01	< 0.01	< 0.01	13.44	13.03	
A-24	MJTE-5	129.2-129.3	pyrite network	0.02	0.15	< 0.01	< 0.01	< 0.01	9.02	10.19	
A-25	MJTE-5	131.2-131.3	pyrite diss	0.35	7.50	2.18	< 0.01	0.02	10.46	11.65	
A-26	MJTE-5	185.2-185.3	powder pyrite net	0.07	1.62	< 0.01	< 0.01	0.01	11.23	12.75	
A-27	MJTE-6	86.9-87.0	pyrite diss tuff	< 0.01	0.49	< 0.01	< 0.01	< 0.01	2.88	2.73	
A-28	MJTE-6	99.2-99.3	pyrite diss tuff	< 0.01	0.88	< 0.01	< 0.01	0.01	4.61	4.24	
A-29	MJTE-6	127.0-127.1	pyrite diss · film	0.02	0.20	< 0.01	< 0.01	< 0.01	12.48	13.09	
A-30	MJTE-6	182.9-183.0	pyrite diss Dc	0.04	0.49	< 0.01	< 0.01	< 0.01	9.41	8.57	
A-31	MJTE-6	194.8-194.9	pyrite diss Dc	< 0.01	0.49	< 0.01	< 0.01	< 0.01	5.18	2.83	qz, py druse
A-32	MJTE-7	148.0-148.4	pyrite network	< 0.01	0.19	< 0.01	< 0.01	< 0.01	10.27	8.72	
A-33	MJTE-7	161.5-161.6	diss py ore	0.03	0.34	< 0.01	< 0.01	< 0.01	21.22	21.77	
A-34	MJTE-7	162.0-162.5	pyrite network	0.01	0.24	< 0.01	< 0.01	< 0.01	11.90	10.14	
A-35	MJTE-7	177.5-177.9	hm+py network	< 0.01	0.29	0.01	< 0.01	< 0.01	6.14	3.92	cp bearing
A-36	MJTE-7	195.9-196.0	diss py ore	< 0.01	0.58	< 0.01	< 0.01	< 0.01	30.14	33.20	
A-37	MJTE-7	198.2-198.4	pyrite diss-net	< 0.01	0.54	< 0.01	< 0.01	0.01	7.87	5.49	
A-38	MJTE-8	82.0-82.1	py+clay vein	0.02	3.46	0.16	0.07	1.50	1.73	1.88	
A-39	MJTE-8	116.4-116.9	arg py net	0.05	4.00	0.12	0.05	0.03	15.74	17.89	
A-40	MJTE-8	124.8-125.0	pyrite diss-net	0.19	2.00	0.02	0.03	0.01	13.06	14.50	
A-41	MJTE-8	142.5-142.7	pyrite diss-net	0.09	0.68	< 0.01	< 0.01	< 0.01	10.94	12.20	
A-42	MJTE-8	188.0-188.2	arg py diss	0.03	< 0.01	< 0.01	< 0.01	< 0.01	8.26	7.93	
A-43	MJTE-8	201.0-201.1	pyrite diss Dc	< 0.01	< 0.01	< 0.01	< 0.01	< 0.01	5.76	4.41	

Abbreviation
py:pyrite, cp:chalcopyrite, sph:sphalerite, hm:hematite, Dc:dacite,
diss:dissemination, net:network, arg:argillization, sil:silicification

Table II-4-1 Results of the Chemical Analysis of Core Samples (2)

NO.	DRILLING NO	DEPTH (m)	SAMPLE TYPE	Au (ppm)	Ag (ppm)	Cu (%)	Pb (%)	Zn (%)	FE (%)	S (%)	REMARKS
A-1	MJTE-9	138.5(25cm)	py-film+diss dc	0.18	0.69	< 0.01	< 0.01	0.01	1.69	1.61	
A-2	MJTE-9	224.0(20cm)	arg.py-diss	0.09	0.93	0.01	0.18	0.06	2.83	2.01	
A-3	MJTE-9	227.0(30cm)	cp+sph.py breccia	0.06	1.17	0.15	0.01	1.32	6.33	5.69	
A-4	MJTE-9	227.6(10cm)	cp-sph.py vein	0.06	7.10	4.16	0.21	4.66	7.99	10.80	
A-5	MJTE-9	248.8(10cm)	gn.sph.cp-vein	0.14	8.64	0.38	0.01	4.34	9.57	5.54	
A-6	MJTE-10	103.0(10cm)	py arg-zone	0.20	0.65	< 0.01	0.01	0.03	1.99	1.93	
A-7	MJTE-10	104.5(20cm)	py weak net	0.04	0.74	< 0.01	< 0.01	< 0.01	6.73	7.90	
A-8	MJTE-10	105.0-105.5	py-net/diss	0.08	0.70	< 0.01	< 0.01	0.01	3.85	4.32	
A-9	MJTE-10	124.5(30cm)	py-film dc	0.19	0.51	< 0.01	< 0.01	0.01	3.11	2.94	
A-10	MJTE-10	181.5(50cm)	py+cal net	0.05	0.48	< 0.01	< 0.01	0.01	3.65	3.18	
A-11	MJTE-10	206.0(30cm)	py-net	0.11	0.79	< 0.01	< 0.01	< 0.01	2.17	1.50	
A-12	MJTE-10	225.5(30cm)	sil.py-net	0.18	1.17	< 0.01	< 0.01	0.01	1.44	1.49	
A-13	MJTE-10	229.5(25cm)	py-net	0.10	0.89	< 0.01	< 0.01	0.01	1.32	1.11	
A-14	MJTE-10	232.3(20cm)	breccia fill py	0.15	1.17	0.01	< 0.01	0.02	4.74	5.65	
A-15	MJTE-10	238.5(50cm)	arg.py zone	0.26	2.94	0.10	0.20	0.18	5.86	6.87	
A-16	MJTE-11	20.5-22.5	arg.fine py zone	0.08	0.89	< 0.01	< 0.01	< 0.01	4.38	4.43	
A-17	MJTE-11	44.0-45.0	breccia filling py	0.15	1.07	0.01	< 0.01	< 0.01	5.20	5.43	
A-18	MJTE-11	51.0-52.0	arg-py>cp	0.18	1.17	0.04	< 0.01	0.01	3.71	3.62	
A-19	MJTE-11	78.0-79.0	py net cp bearing	0.38	0.82	0.17	0.01	0.02	8.35	10.33	
A-20	MJTE-11	79.0-80.0	py net cp bearing	0.17	1.36	0.13	< 0.01	0.01	7.60	7.82	
A-21	MJTE-11	86.0-87.0	arg.py diss	0.14	0.98	< 0.01	< 0.01	0.02	6.18	6.95	
A-22	MJTE-11	180.0-180.5	arg with py	0.44	5.23	0.06	0.04	0.20	3.41	3.89	
A-23	MJTE-11	202.0-202.5	sph+cp net	0.24	2.20	0.20	< 0.01	1.46	1.48	2.23	
A-24	MJTE-12	24.3-25.0	coarse py massive	0.08	1.59	0.01	0.01	0.03	35.69	39.08	
A-25	MJTE-12	25.0-26.5	py.sil net/arg	0.07	1.17	< 0.01	< 0.01	< 0.01	14.51	15.77	
A-26	MJTE-12	34.6-35.6	py net/diss	0.10	1.03	< 0.01	< 0.01	< 0.01	26.23	30.01	
A-27	MJTE-12	49.0-50.0	joint filling py	0.10	0.65	< 0.01	< 0.01	< 0.01	23.78	27.20	
A-28	MJTE-12	85.0-85.5	py diss/net	0.13	0.70	< 0.01	< 0.01	< 0.01	31.81	37.00	
A-29	MJTE-12	202.0-203.0	arg with py	0.34	0.98	0.01	< 0.01	< 0.01	5.65	6.34	
A-30	MJTE-12	211.0-212.0	py+clay net	1.63	9.77	0.11	0.02	0.70	7.28	8.53	
A-31	MJTE-12	218.0-218.5	py net cp bearing	0.87	5.05	0.07	0.10	1.39	10.96	6.87	
A-32	MJTE-12	222.8-223.8	arg with py	0.26	4.02	0.01	0.01	0.19	6.73	3.80	
A-33	MJTE-12	345.5(50cm)	py net	0.09	2.85	< 0.01	< 0.01	0.02	2.56	1.30	

Abbreviation

py:pyrite, cp:chalcopyrite, sph:sphalerite, hm:hematite, Dc:decite,
diss:dissemination, net:network, arg:argillization, sil:silicification

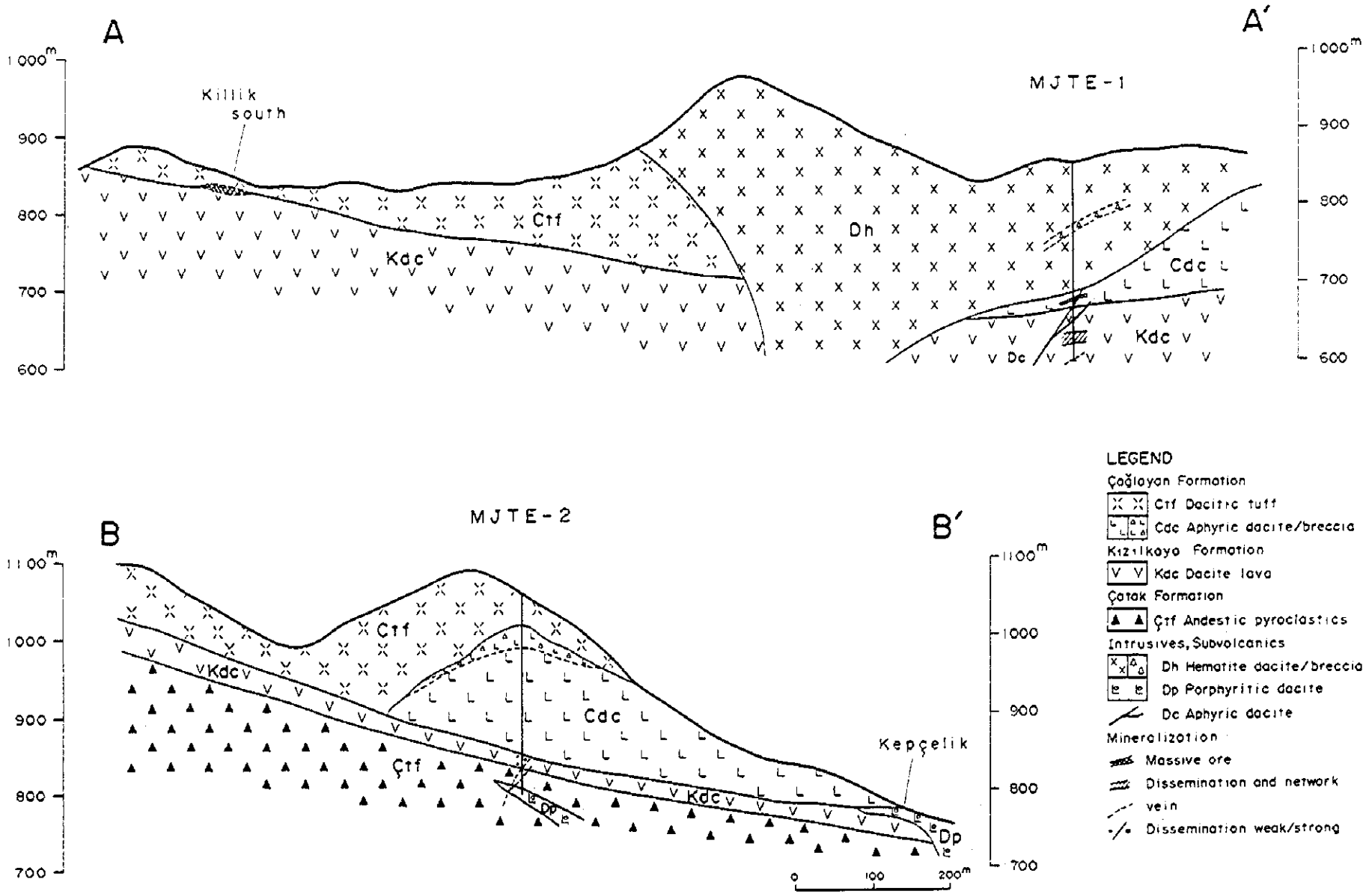

Fig.II-4-3 Geological Sections (MJTE-1, MJTE-2)

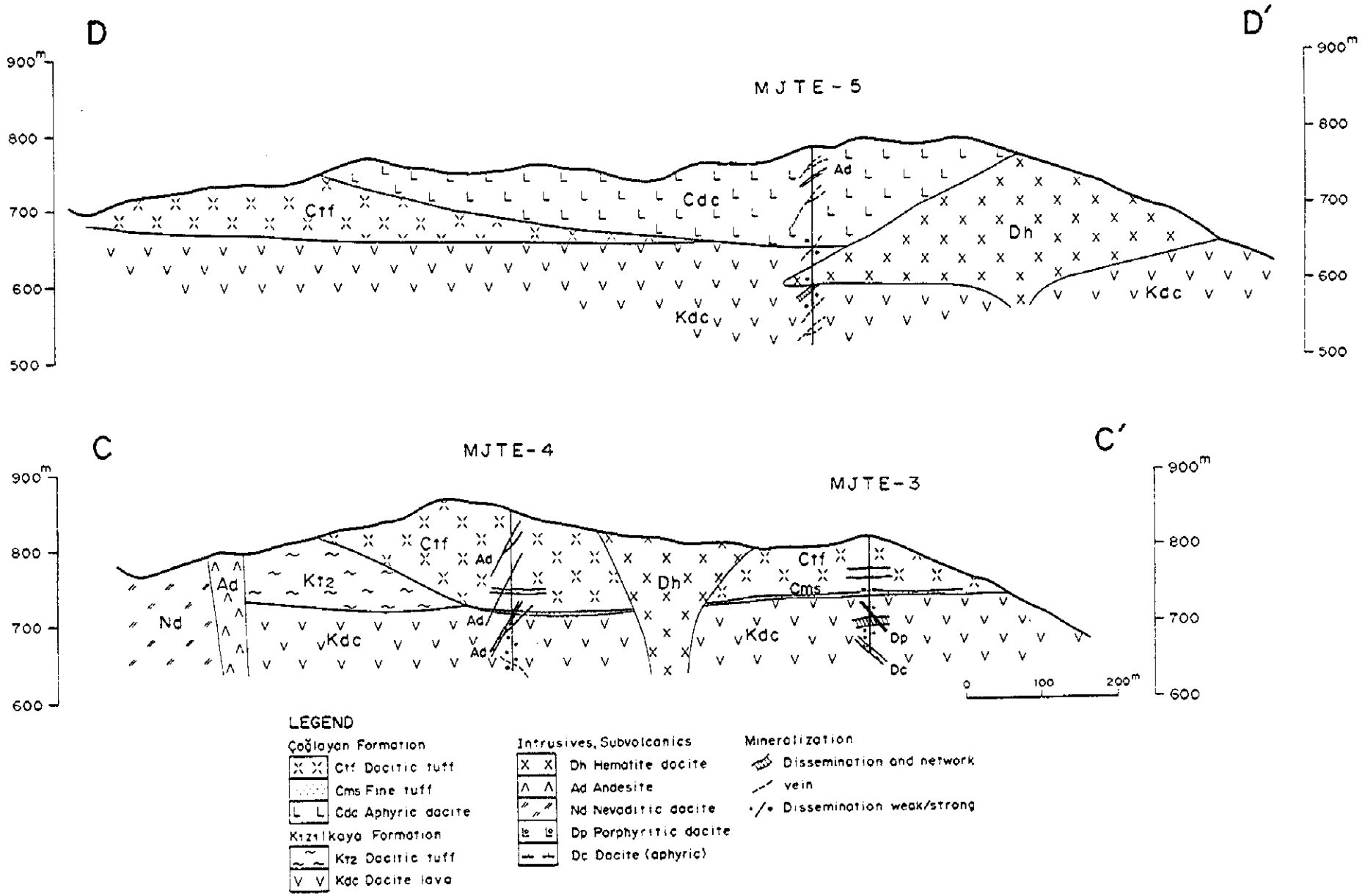

Fig.II-4-4 Geological Sections (MJTE-3, MJTE-4, MJTE-5)

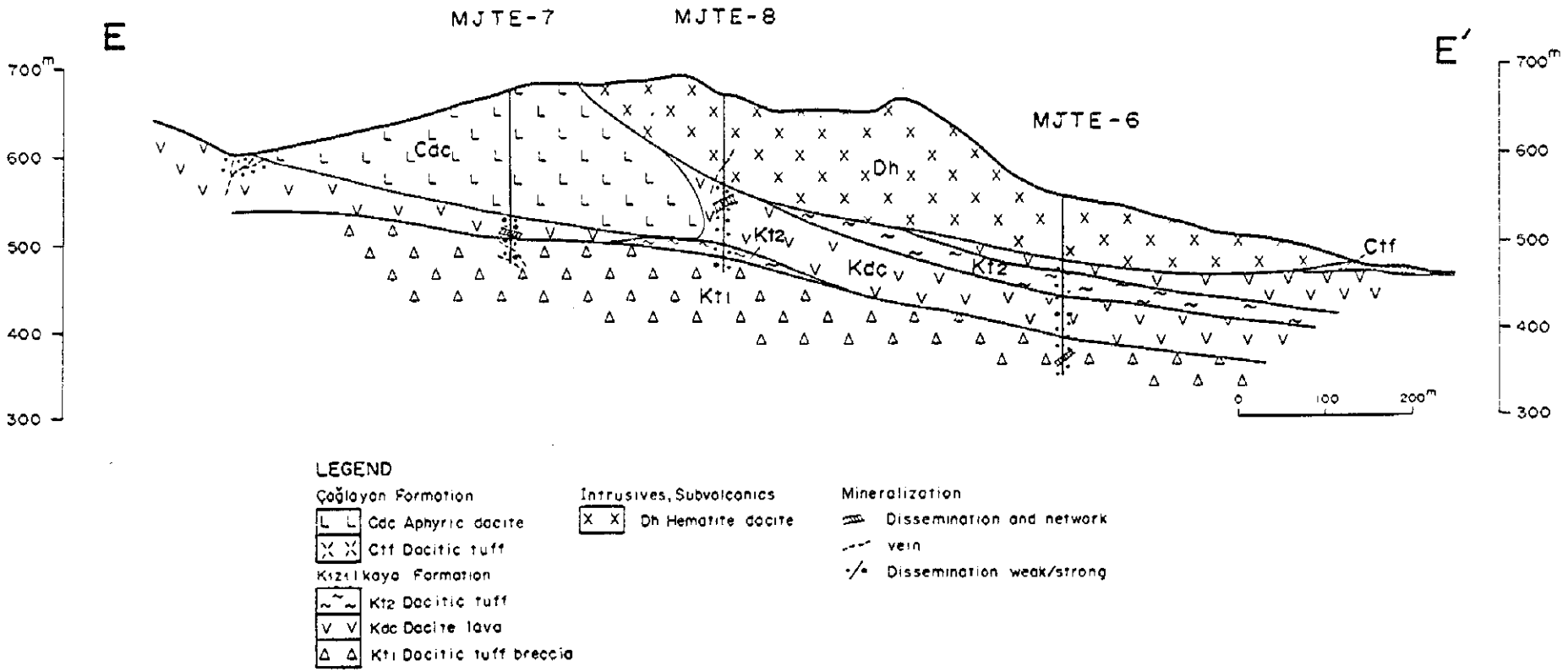

Fig.II-4-5 Geological Section (MJTE-6, MJTE-7, MJTE-8)

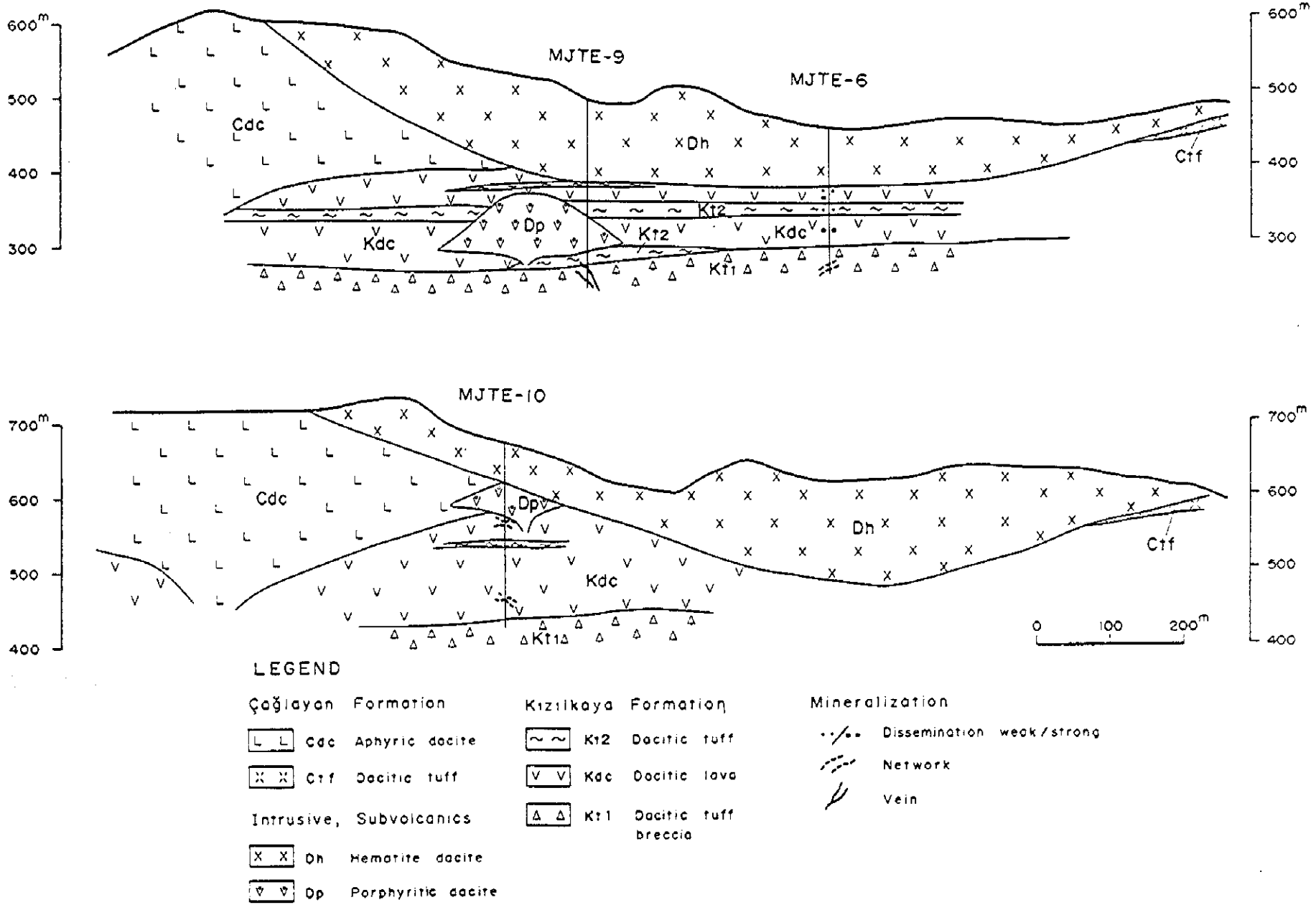

Fig.II-4-6 Geological Sections (MJTE-9, MJTE-10)

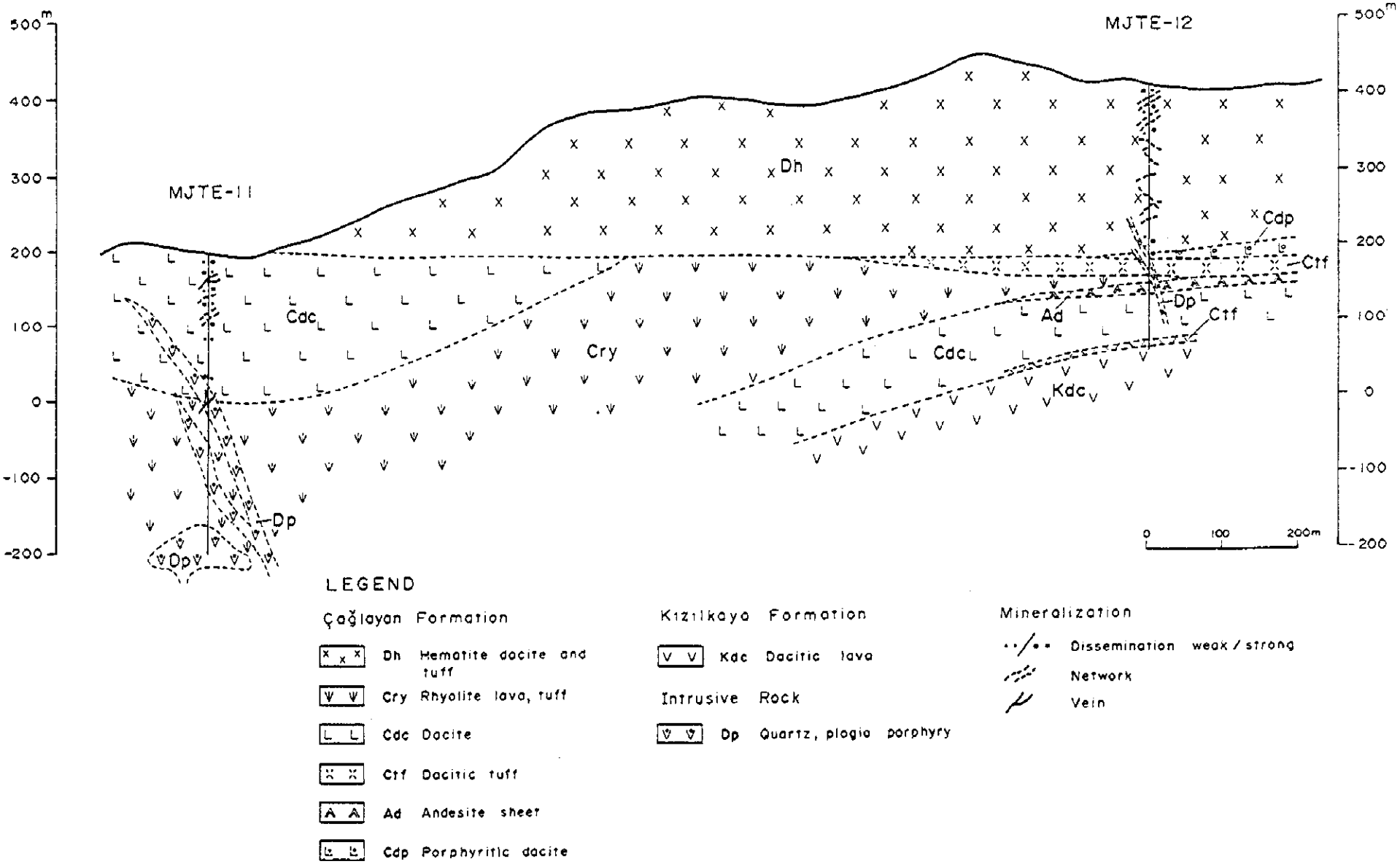

Fig.II-4-7 Geological Section (MJTE-11, MJTE-12)

Chapter 5 General Discussion on Survey Results

5-1 Characteristics of Geological Structure and Mineralization, Mineralization Restrictions

As already mentioned above, the coastal zone of eastern Black Sea Region including the survey area is occupied by volcanic rocks of Late Cretaceous accompanied by massive sulfide and similar mineralized zones. The massive sulfide deposits in eastern Black Sea Region are hosted in particular horizon, and it is considered that deposits were formed under the similar geological and structural environment as Japanese kuroko depositqs since the ore resemble to Japanese kuroko, even though the formation was different.

In this area, ore horizon of the massive sulfide deposits such as Lahanos, Killik and Kızılkaya deposits is situated on the top of the Kızılkaya Formation and is covered by tuff and hematite dacite of the Çağlayan Formation. In particular, hanging wall tuff of the Çağlayan Formation contains plenty of greenish volcanic glass and has considerable thickness compared to the other deposits, ore showings. Therefor, relatively thick distribution of hanging wall tuff may keep the large sized ore body after it's deposition.

The alteration zone mainly of sericite has occurred in footwall dacite as mineralization halo, and in the vicinity of Lahanos deposit or so, the alteration zone continues up to the hanging wall, accompanying kaolinite. Also, Karılar deposit or so in the north region is considered to be network mineralization consisting mainly of coarse pyrite and formed later than the massive sulfide deposit, but the alteration is consisting mainly of sericite and kaolinite and quite similar with the alteration of hanging wall of Lahanos deposit. Moreover, since recrystalized form of colloform pyrite into coarse pyrite has been observed, it is considered that repeated hydrothermal activities possibly occurred in very wide area. With this reason, it seems rather difficult to detect apparent geochemical characteristics of hanging wall and footwall by geochemical survey.

5-2 Relationship between Geophysical Survey Results and Mineralization

As the result of gravity survey, it is clearly shown that regional gravity trend of NE to ENE system is predominant both of structure along the same direction and smaller structure of NW system diagonally crossing with the direction. Also, because it can be considered that igneous activity since Cretaceous has related with deep fracture of EW to NE system, it is highly possible for the mineralization at this area to have relationship with the structure along the same direction.

Gravity structure in this area is not so clear but there is tendency that the mineralized zones including Lahanos, Killik, Kızılkaya, Taflancık and Çalkaya deposits are distributed in low gravity zone of NE system, and also coincide with sericitization zone of footwall. This alteration zone continues to northeast direction outside the area and is covered by the hanging wall in its midway, and, moreover, it is known that a group of massive sulphide deposits and mineralized zones is situated in Tirebol area.

Contrary to this tendency, Karacrik, Karılar and Ağalık deposits belonging to northern deposit group are located at peripheral area of high gravity zone of NNE system. The Ağalık deposit is possibly massive type deposit but Karacrik and Karılar deposits have been considered to be vein-network type deposit of late stage. Since porphyritic dacite intrusive has been encountered often in the drilling the high gravity zone is possibly to be concealed intrusive.

The IP survey had been conducted during 3 years for promising area selected through consideration of geology, alteration and mineralization. Consequently, new IP anomaly zones were found in Killik and Taflancık areas. Since IP anomaly zone was recognized widely at footwall dacite, dissemination-stockwork type mineralization zone was presumed, but massive ore body could not be expected. At Taflancık area, IP anomaly zone was found in a deep part of the area covered by hanging walls. By the survey results of 5 drillings conducted at this anomaly zone, intense dissemination-vein type mineralization was partially recognized and also fragments of high grade yellow ore were recognized. In this way, it was clearly understood that the IP anomaly reflects mineralization of massive deposit type, however, no ore body was discovered so it was considered that massive ore body might be eroded out. The measured chargeability is lower than 20mV/V. If large sized ore body could exist, indication of lower resistivity and higher chargeability is much more preferable to confirm it.

For the IP survey conducted in Karılar area, the IP anomaly well reflecting the shape of existing Kararik and Karılar deposits was detected probably by the reason using 2 dimensions Inversion program. Observed maximum chargeability was 30mV/V or so. With the means applying these analytical procedures, it would probably be possible to discover new deposit by the IP survey if large sized massive ore body could exist in the survey area.

5-3 Potential of Ore Deposit

Large sacale of ore deposit will be expected in a mineralized zone including Lahanos-Kızılkaya deposit and extending towards NE direction, if relatively thick hanging wall tuff (containing a plenty of greenish glass) and hematite dacite will distribute with considerable thickness.

Bitene area is located south of Lahanos deposit and satisfies the conditions mentioned above. Drilling result at Bitene area (MJTE-3) shows existence of massive yellow orebody (Cu 12.58%, Au 2.06ppm) even though the thickness is only 20cm. However, from the result of MJTE-4 and also geological and geographic conditions, it was judged that there is little possibility of existence of economical ore body

Çalkaya area satisfies fundamental conditions mentioned above but, in the result of geophysical survey (IP method, a=100m) in phase II, any apparent anomaly was not reported. Since thick hanging wall distributed over the areas from Çalkaya area to Taflancık area and thus exploration depth of the IP survey would be probably not enough, clear indication of mineralization

at very deep part would be probably detected by IP survey of a=200m, for example.

Kartlar and Karaerik deposits at northern part were considered to massive type mineralization of the same horizon as Lahanos deposit, but it was clearly indicated that those deposits were formed in late stage. In the coastal zone of Eastern Black Sea, it was widely said that the mineralization related to dacite of Late Cretaceous was often treated as massive sulfide mineralization, and the possibility of vein-stockwork mineralization of late stage was very scarcely reviewed up to date.

Potential zone of the massive sulfide ore deposits might be increase in the Eastern Black Sea Metallogenic Province, if the results of this survey were applied

PART III Conclusion and Recommendation

PART III Conclusion and Recommendation

Chapter 1 Conclusion

After the existing data was analyzed, the surveys such as geological survey (including ore showing survey and geochemical survey), geophysical survey (gravity method, IP method and CSAMT method) and drilling survey were carried out. Comprehensively analyzing the results of these surveys, the following conclusions were obtained.

In the surveyed area, there are a number of ore showings and ore deposits including the Lahanos mine (under operation). Before this project, all of these existing ore deposits and ore showings are considered relating to the massive sulfide type mineralization, but it has been clarified that at least the ore deposits located in the north part were formed by the newer stockwork mineralization like the cases of Karılar and Karaerik ore deposits.

The massive sulfide type ore deposits such as that of Lahanos were formed relating with acidic volcanism in late Mesozoic. The massive sulfide type ore deposits are hosted in the top of the Kızılkaya Formation and covered with the tuff and hematite dacite of the Çağlayan Formation. The massive sulfide ore body is accompanied by intense argillic alteration, mainly the sericitization and frequently accompanying the kaolinite. Such alteration was continued to the hanging wall even after the formation of the ore body in the cases of Killik and Lahanos ore deposits.

Based on the result of the geochemical survey of the rock, it is considered that the high score zone of the second principal component reflected well the mineralization.

Through the sub-regional gravity survey, it was clarified that, the gravity trend in NE-SW or ENE-WSW direction was predominant around this area, and the bouguer anomaly rises towards the Black Sea, and many of the existing ore deposits distribute in the surrounging areas of the high gravity zone.

It is considered that the IP method is the effective method for the areas covered with hanging wall. That is, new anomaly zone reflecting mineralization was found in Taflancık area. And also in the Karılar area, the observed anomaly reflected well the form of ore body.

Resistivity structure (ENE-WSW trending) related to mineralization was found by the CSAMT method in Karılar area.

The drilling survey was carried out at 12 sites of selected promising area during the second year and third year surveys. As the results of these drilling surveys, a massive yellow ore (Cu 12.58%, Au 2.06ppm) of 20cm thick was found at MJTE-3 in Bitene area, and yellow ore fragments were encountered at MJTE-6 in Taflancık area. Further, in other drilling sites too, pyrite dissemination zones and stockwork mineralization zones including chalcopyrite, pyrite and sphalerite were observed, and a wide distribution of mineralization zone relating to the massive sulfide ore deposit was also clarified. The major mineralization zone is a zone including Lahanos

and Kızılkaya ore deposits and is considered extending to the northeastern direction.

Chapter 2 Recommendation in the Future Projects

1. Survey at greater depth by IP method and drilling survey in Çalkaya area.
2. Detail study for footwall dacite and reexploration (checking) of the massive sulfide type ore showings in the Black Sea Region.

References

References

Çagtay,M.N. (1993) :Hydrothermal Alteration associated with Volcanogenic Massive Sulfide Deposits: Examples from Turkey, Economic Geology, 88,606 -- 621.

Coggon J.H (1971) :Electro magnetic and Electrical Modeling by Finite Element Method. Geophysics,Vol.36,No.1,115-132

Demir Export A.Ş (1990) :Lahanos Bakir-Çinko Yatagında Yapılan Arama Ve Değerendirme Çalismaları.

Demir Export A.Ş (1994) :16.03.1988 Tarihli Anlaşma Kapsaminda Giresun-Espiye ve Tirebolu Sahalarında Yapılan Arama Çalısmalariyla Ilgili Faalıyeyet Raporu Geological Survey of Japan (1993) :Cishitu News, No.467, 69P.

Güven,I.H., Serdar,A.H.,Er.M. and Özdoğan, K. (1992) :Mineral Deposits and Metalog enic Zonality of the Eastern Pontides Magmatic Arc, NE Turkey. Procee dings of ISGB, P.61.

Inoue,Eiichi (1970) :Geologic Outline of Turkey, Proceedings of MIneral Resources Information Center of MMAJ, No.15, P1-P34. (in Japanese)

Kato, Hirokazu (1991) :Pull-Apart Basin in Eastern Turkey. Structual Geology,No.36, P65-75.

Kormaz, S., Er, M., Van,A.,Musaoğul,A.,Keskin,I. and Tuysuz,N. (1992) :Stratigraphy of the Eastern Pontides, NE-Turkey. Proceedings of ISGB, P.17.

M..Ymashita and Y.Ogawa (1993) :CSAMT case histories with a multichannel CSAMT system and discussion of near-field data correction. Thee 55 th SEG Meeting,Washington,D.c.

Murat Erendil (1993) : Geolgical Setting of Anatolia. Chishitu News No.467,P11-20. (in Japanese)

Rijo Luiz (1977) :Modeling of Electric and Electromagnetic Data. PhD.Thesis. University of Utah.

T.Uchida and Y.Ogawa (1993) :Development of Fortran Cord Two-dimensional Magneto-telluric Inversion with Smoothness Constraint. Geological survey of Japan, Open-File Report, No.205, pp115